General report/Discussion session 1: Recent developments in laboratory strength and deformation testing

Rapport de spécialistes/Séance de discussion 1: Développements récents de mesure en laboratoire de la résistance et de la déformation des sols

YUDHBIR, Indian Institute of Technology, Kanpur, India & AIT, Bangkok, Thailand
D. MUIR WOOD, Glasgow University, Scotland, UK

SYNOPSIS: Recent developments in laboratory strength and deformation testing are discussed against a background of the need to understand the purpose for which testing is required before performing that testing. Developments are discussed in automation and instrumentation of equipment, in apparatus; in techniques of sample preparation, in understanding of time effects, and changes in particulate structure of clay and quantification of particle shape of sands; in interpretation of experimental data through methods of presentation of results, through description of the yielding of soils, through changes in sand gradation and particle shape during testing, through the use of a state variable to bring together information of volumetric packing, stress level, grain angularity and gradation in understanding the behaviour of sands, and through generalized relationships to describe the behaviour of clays in remoulded and resedimented states.

1 INTRODUCTION

It has not seemed appropriate to prepare anything approaching a state-of-the-art report on this subject for this present conference because such a comprehensive report was produced by Jamiolkowski et al (1985) for the 11th International Conference on Soil Mechanics and Foundation Engineering held in San Francisco. Rather, this report attempts to note some of the areas where developments have taken place or are taking place, to note some of the areas where developments still need to take place, and to note how the papers submitted to this session match up with these areas.

The coverage is inevitably partial both in the sense that, with the background of the 1985 report, it does not attempt to describe comprehensively all aspects of laboratory strength and deformation testing, and in the sense that it reflects the prejudices and interests of the authors. No particular apology is therefore made for neglecting certain topics which may be dear to certain readers.

2 PURPOSE OF TESTING

Laboratory testing can not be performed in a conceptual void but only against the background of some intended application. The range of intended applications can be large. At one extreme a practising engineer may require values of soil strength or stiffness to insert into a well-tried design formula. Such a person may not be particularly keen on new methods of measuring strength or stiffness because the design formulae have themselves usually grown up in association with traditional testing techniques. Although new techdnigues may produce values of soil parameters which the experimentalist regards as "more accurate" it may be that this extra accuracy removes a necessary conservative margin of error (or ignorance) in the design formula - new wine should not be put in old bottles.

At the other extreme, the research engineer may require particularly subtle tests in order to validate the hypotheses on which a particular new constitutive model of soil behaviour is based. For such an application it will be particularly important that the experimental standards are of the highest since, although it is clear that all experimental observations are true, it is desirable that in selecting data to support a particular soil model the margin of flexibility in interpretation of this truth should be as small as possible.

In between there are many users of laboratory testing who are attempting to do unusual engineering for which existing rules of thumb provide only a shaky basis. These people also will be using models of soil behaviour - either explicitly or implicitly- in design calculations or numerical analyses, and will be concerned to know not only what soil parameters to use in these models, but also whether there are aspects of soil behaviour that have traditionally been neglected that could be significant in their particular situation.

To talk only about strength and stiffness testing of soils would be to assume that soil behaviour could be described by the simple dashed bi-linear shear stress-strain relationship shown in Fig. 1. No real soil behaves in this way, and the use of the term deformation testing in the title makes it clear that it is the more general pre-failure behaviour of soils that is of interest as indicated by the solid curve in Fig. 1: a single stiffness is not sufficient to describe this behaviour, which requires a complete constitutive soil model. A single strength will probably also not be sufficient - certainly not without some reference to a soil model in which it is to be

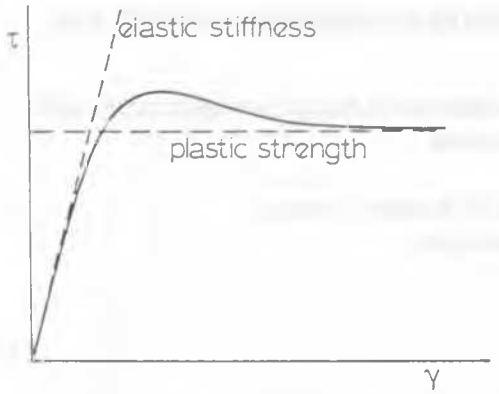

Figure 1. Idealised and actual stress-strain relationships.

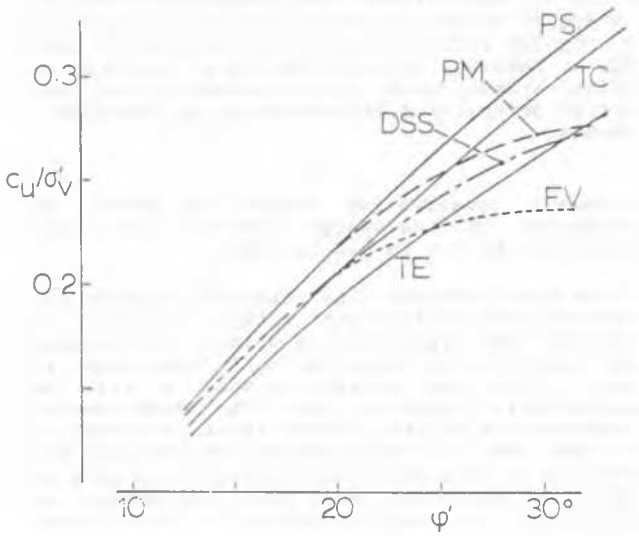

Figure 2. Dependence of undrained strength on test method (PS: plane strain; TC: triaxial compression; PM: pressuremeter; DSS: direct simple shear; FV: field vane; TE: triaxial extension).

incorporated. In particular, it is well known that the measured undrained strength of soils is dependent on the method of measurement - this was emphasised by Wroth (1984) with especial reference to in situ testing and is illustrated in Fig. 2 with calculations made using the modified Cam Clay model (Roscoe and Burland, 1968) combined with a Mohr-Coulomb failure criterion. Though this particular model may not be regarded with great favour this example does demonstrate the way in which an effective stress model of soil response can help to make sense of undrained, total stress, measurements.

There is no session dedicated to constitutive models of soils in this conference - there are other conference series which deal more exclusively with this subject (see Swoboda (1988) and Pietruszczak and Pande (1989) for a couple of recent examples). However, as soon as one enters the area of deformation of soils,

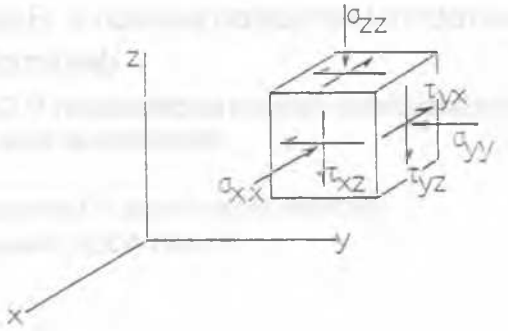

Figure 3. General stress systems.

understanding of behaviour of soils under working loads, then some feel for constitutive modelling becomes extremely important.

A constitutive model is a basis for extrapolation from an experimental data base towards the unknown region of soil response in a particular unusual type of boundary value problem. For such extrapolation to be credible the experimental data base needs to be as wide as possible. A stress state in an element of soil is described by six independent quantities - for example, the normal stresses and shear stresses on three mutually orthogonal sets of planes (Fig. 3). The range of stress paths that may be experienced by soil in the ground will be infinite and in order that laboratory testing should be able to explore this infinity as far as possible the laboratory test devices would ideally need to provide control of six independent degrees of freedom. Such a large number of freedoms is unlikely ever to be available in single element testing and some degree of extrapolation will always be inevitable. The present possibilities are summarised in Table I.

The term "single element" has been used and it is certainly convenient if the laboratory specimen that is being tested can be treated as a uniform homogeneous single element. Developments in testing equipment and techniques may on the one hand move in the direction of trying to ensure that a sample is loaded and deforms

Table 1. Testing Possibilities.

Apparatus	Number of degrees of freedom
1. With fixed principal axes	
1.1 Oedometer	1
1.2 Triaxial apparatus	2
1.3 Biaxial (plane strain) apparatus	2
1.4 True triaxial apparatus/ cubical cell	3
1.5 Hollow cylinder apparatus	3
2. With rotation of principal axes	
2.1 Shear box	2
2.2 Simple shear apparatus	2
2.3 Directional shear cell	3
2.4 Hollow cylinder apparatus	4

as uniformly as possible so that it can indeed be treated as a single element, or may on the other hand accept that the laboratory test is at best a rather simple boundary value problem and attempt to instrument the test in such a way that the response of an equivalent ideal uniform sample can be deduced.

Of the testing possibilities listed in Table 1, the shear box is clearly not a single element test - no pretence is made at forcing uniform deformation of the soil. The simple shear apparatus is also flawed but can be instrumented (see for example, Stroud, 1971) in order to try and escape into the sample and away from the source of the non-uniformities. The hollow cylinder apparatus - which with control of internal and external pressures, axial load and torque provides an impressive four degrees of freedom - unfortunately cannot escape radial non-uniformity. Even with identical internal and external pressures which, while reducing very severely the region of stress space that can be explored, does encourage more radial uniformity of stress, there is inevitably a radial variation in shear strain and tests in this device have to be interpreted through average stress and strain quantities (Hight, Gens and Symes, 1983) or else the raw data of torques and loads incorporated into a back-analysis of the boundary value problem.

More or less extensive discussion of the use of some of the testing apparatus listed in Table 1 is contained in the book edited by Donghe et al (1988) which deals primarily, but by no means exclusively, with advances in conventional triaxial testing.

3. DEVELOPMENTS IN EQUIPMENT

There are three main areas in which equipemnt developments are taking place. There is an increased use of automation in driving conventional testing apparatus. New instrumentation is being developed to monitor the performance of soil samples. New apparatus are being developed to extend the range of soil characteristics that can be explored.

3.1 Automation

Many years have passed since Lambe (1967) described his stress path method for estimating settlements of geotechnical structures. This should have been the prompt to the geotechnical community to perform more relevant laboratory testing but the reaction time has in general been rather slow. Of course, the triaxial apparatus is not able to match the actual stress changes that are likely to occur at most elements in the ground (except under the centre of a circular tank) and plane strain conditions are of more frequent occurrence than axial symmetry. Nevertheless it is not necessary to use only conventional triaxial compression tests if simple consideration of a field loading situation suggests that this is completely inappropriate - and a conscious choice should be made of the model to be used to perform the extrapolation from axially symmetric to plane strain conditions.

A good example of the inappropriateness of conventional testing is provided by Brand's (1981) discussion of the stress path involved in rain induced slope failure: a frequent cause of landslides in tropical areas. The in situ stress conditions are not simple (the principal axes will not be vertical and horizontal) and the deformations that accompany infiltration may occur approximately under conditions of plane strain, but Brand suggests that the effect of infiltration of surface rainfall will be to reduce pore suctions without changing the total stresses significantly. The relevant closest approximation to this stress path that can be applied in the conventional triaxial apparatus is shown in Fig. 4 : reduction in mean effective stress $p' = (\sigma_a' + 2\sigma_r')/3$ with constant deviator stress $q = \sigma_a' - \sigma_r'$. This is markedly different from the conventional triaxial compression test performed with constant radial stress and hence $\delta q/\delta p' = 3$ (shown dotted in Fig. 4). A rare set of tests exploring cyclic loading along such a constant q stress path is reported by Eigenbrod et al (1987) who were concerned to study the possibility of failure being reached in a slope at low effective stresses due to seasonal variation of pore pressure.

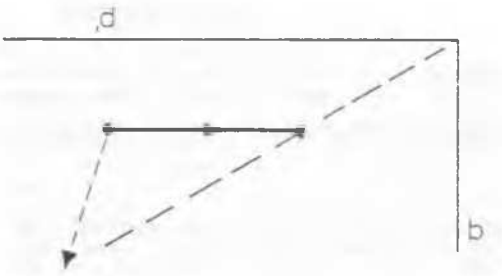

Figure 4. Effective stress paths in triaxial plane.

Some of the resistance to choosing relevant stress paths has come because current design procedures are based on the results of conventional tests. Some of the resistance has come because performance of other paths requires some sort of feedback control which used to be extremely labour intensive but is now straightforward because a vast range of microcomputers and electronic devices has become available over the last decade. Unavailability of equipment can no longer be accepted as an excuse for not performing relevant tests.

There are a number of different commercially available computer-controlled triaxial apparatus and many laboratories have produced their own versions. Different methods of control have been used depending, principally, on whether axial stress or axial strain is directly controlled (rather than indirectly controlled by feedback). Direct stepper motor control of axial deformation has been used by Houlsby (1981) and by Kolisoja et al (1989) and Olli et al (1989). Control of axial stress using an electro-pneumatic transducer is the principle adopted by Li et al (1988) and Shen et al (1989). Vaid et al (1988) have a choice either of stress control by controlling the pressure acting on a piston in an axially-mounted

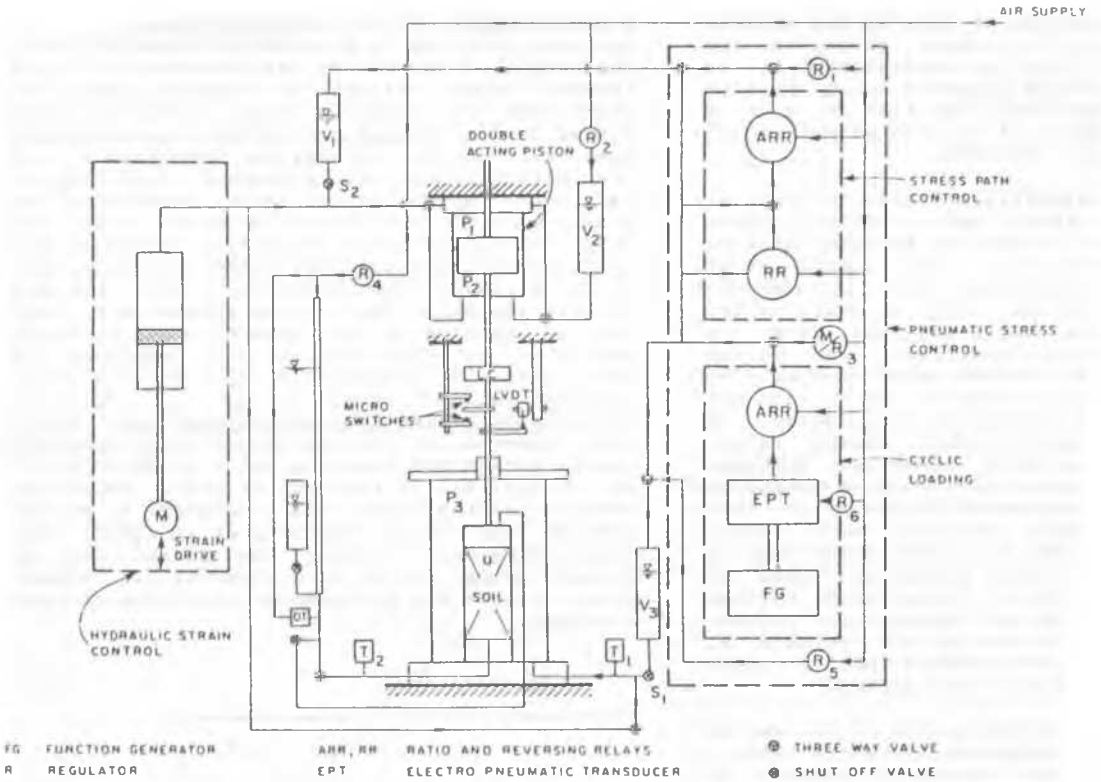

Figure 5. Diagram of triaxial loading system (from Vaid et al, 1988).

cylinder or of strain control by controlling the rate at which water is pumped into the cylinder (Fig. 5). This mode of control is particularly suited to the hydraulic triaxial cells described by Bishop and Wesley (1975) and it is these cells which are combined with particularly sophisticated pressure/volume controllers in the system described by Menzies (1988).

There is less choice of method for applying the radial cell pressure-most people adopt some variant of an electro-pneumatic transducer. The back pressure/volume change system requires simultaneous control and measurement of volumes and pressures either in separate devices or using the single combined controller described by Menzies (1988).

The choice between systems may be largely a matter of personal preference and will be linked with the type of testing that is to be performed. Feedback response times can be sufficiently rapid that even a sharply strain softening resposne such as that shown in Fig. 6 - which would traditionally have been expected to require strain control - can be followed with the stress-controlled apparatus of Shen et al (1989).

3.2 Instrumentation

Traditionally triaxial samples were assumed to deform uniformly so that measurement of pore pressure at the ends of the specimen, overall axial strain measurement, and deduction of radial strain from overall volume change could be assumed to give representative values. With the recognition that uniformity is less inevitable than had been supposed attempts were made to encourage uniformity by reducing end friction (Rowe and Barden, 1964). Use of lubricated end plates, however, would require special attention in the elimination of the associated bedding errors. (Goldscheider, 1982; Kolymbas & Wu, 1989).

More recently the non-uniformity has been accepted and instrumentation devised to measure pore pressures at mid-height, to measure axial strains over a central gauge length that is "remote" from the ends of the specimen, and to measure radial strains directly in the central part of the specimen (Fig. 7). General discussions of the ways in which these measurements can be made may be found in the papers by Tatsuoka (1988) and Baldi et al (1988), (see also, Kolymbas & Wu, 1989).

It may be noted that there are many different systems available for local deformation measurement - most of which can be adopted to measurement of either axial or radial deformations. In Britian, for example, there are research groups using electrolevels (Jardine et al, 1984), Hall effect semiconductor devices (Clayton and Khatrush, 1986), and proximity gauges (Hird and Yung, 1987) - and no doubt there are other systems too. The requirement to be able to find space to suspend such instrumentation around the soil sample inside the cell carries with it a need for larger diameter cells to become more standard (see, Kolymbas & Wu, 1989).

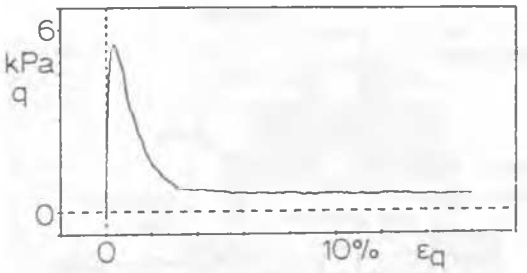

Figure 6. Strain softening response in undrained compression test on loose sand (I_D= 5%, σ_v = 100 kPa) (from Shen et al, 1989).

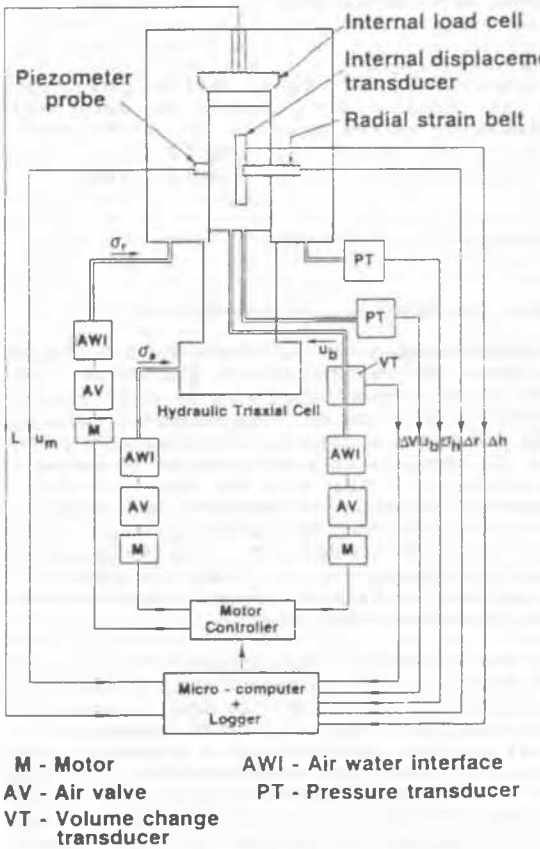

Figure 7. Imperial College triaxial testing system (from Baldi et al, 1988).

3.3 Apparatus

The range of existing testing possibilities was reviewed at the end of section 2. The least familiar apparatus in that list is probably the Directional Shear Cell which permits the simultaneous application of normal and shear stresses to the sides of an initially cuboidal specimen tested under conditions of plane strain, and allows the soil sample full freedom to deform uniformly under the applied stress system. The first Directtional Shear Cells at University College, London (Arthur et al, 1977) and University of Colorado, Boulder (Sture et al, 1985) (Fig. 8), were restricted to rather low shear stresses so that it was not possible to apply shear stresses of a magnitude that might appeal to civil engineers. However, developments are occurring and the design described by Arthur (1988) (Fig. 9) will improve the possibilities of this type of apparatus enormously, though the complexity associated with this mode of loading and sample freedom is evident in Fig. 8.

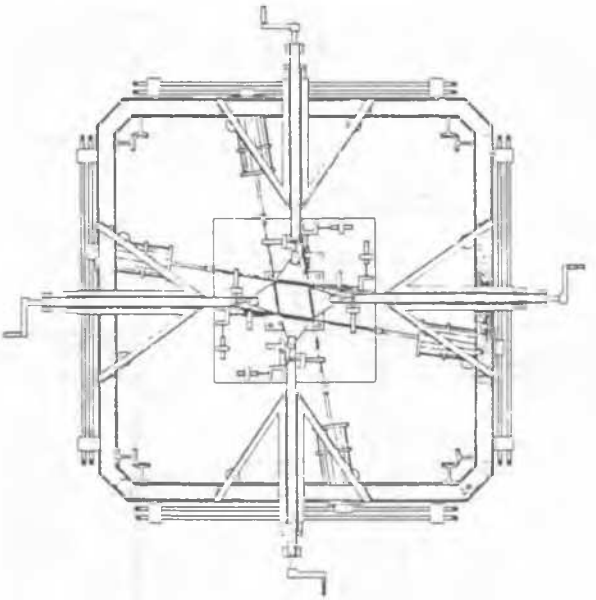

Figure 8. Directional Shear Cell, Boulder (from Sture et al, 1985).

One of the impetus for the development of the instrumentation mentioned in § 3.2 for measurement of strains away from the influence of the ends of a triaxial specimen has been the need to discover the true behaviour of soils at very low strains which can be easily masked by apparatus deficiencies. Low strain stiffness, and the influence of strain level on apparent stiffness can be studied using torsional or axial cyclic shear devices (recent examples have been reported by Wilson (1988) and Van Impe and Van den Broeck (1989)). However a neat way of studying the influence of stress history on small strain shear stiffness of soils is provided by the use of bender elements (Dyvik and Madshus, 1985; Dyvik and Olsen, 1989).

Bender elements are piezoceramic devices which change in shape when subjected to an excitation voltage (Fig. 10), and which correspondingly generate a small voltage when subjected to a change in shape. By incorporating a pair of elements in the top and bottom platens of a soil test apparatus (triaxial, simple shear, oedometer etc) (Fig. 11) a shear wave can be transmitted from one end through the soil to the other and the transmission time directly interpreted as an indication of the shear wave velocity and hence the shear stiffness. The strain level generated by the transmitting element is less than 10^{-3}% so that the stiff-

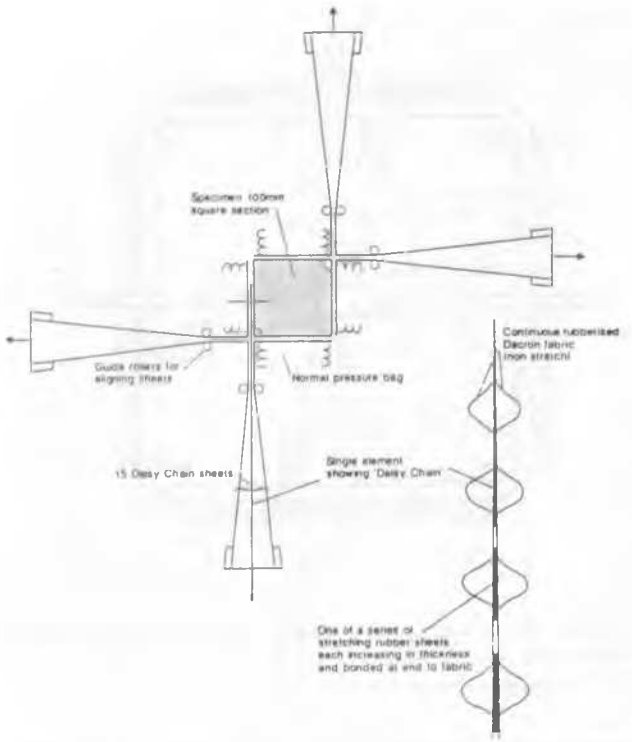

Figure 9. UCL Directional Shear Cell with daisy chain shear sheets to increase range of applied shear stresses, (from Arthur, 1988).

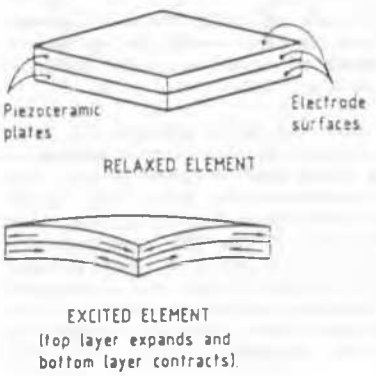

Figure 10. Shape of piezoceramic bender elements with and without applied excitation voltage (from Dyvik and Madshus, 1985).

ness that is measured may reasonably be regarded as a truly elastic property. Dyvik and Olsen (1989) show that the moduli measured with bender elements correspond well with those measured by resonant column tests.

It is perhaps not correct to describe the plane strain biaxial apparatus used by Topolnicki (1989) as a recent development (it is essentially the same as the biaxial apparatus used by Hambly and Roscoe (1969)). However, there does remain a stolid preference for conventional triaxial testing even though plane

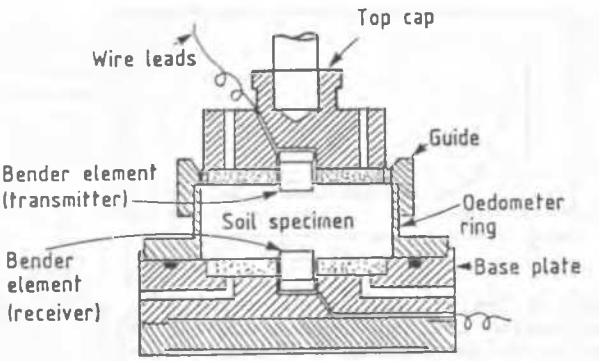

Figure 11. Bender elements mounted in oedometer (from Dyvik and Olsen, 1989).

strain conditions must more realistically represent the constraints imposed on many real soil elements in the ground. It seems that there is still a need for an easily used plane strain test apparatus of the biaxial type.

4 DEVELOPMENTS IN TECHNIQUES

4.1 Sample preparation and homogeniety

As the understanding of the behaviour of soils in the field and the laboratory increases and accuracy of measurement improves so the search for possible sources of discrepancy between field and laboratory observations has to intensify and all aspects of testing have to be examined carefully. The need for more accurate measurement of strains has already been referred to, but accurate measurements are only useful if they can be related to an accurately known desired sample state. Possible disturbances that can be caused by sample preparation procedure need to be removed.

One such disturbance is described by Sladen and Handford (1987) - the change of void ratio of a very loose sand that occurs as the sample is saturated and the triaxial cell is assembled - which they believe may lead to an unconservative assessment of the liquefaction potential of sands. Bressani and Vaughan (1989) suggest that even weakly cemented soil can be disturbed by the process of saturation because of the small cyclic changes in isotropic stress that are implied.

Such observations provide a link with the steadily increasing body of literature on the behaviour of soils under cyclic loading, in this case under stress changes corresponding to cycles of generation and dissipation of pore pressure at constant total stress. Typically such pore pressures will have been generated by cyclic deviatoric loading (for example, Ansal and Tuncan, 1989) but their dissipation will nevertheless result in volumetric compression. Bressani and Vaughan (1989) suggest that another source of disturbance of a soil sample can result from lack of correspondence between top cap and sample, which can lead to non-uniform loading and progressive failrue of the soil structure. The importance of correct alignment

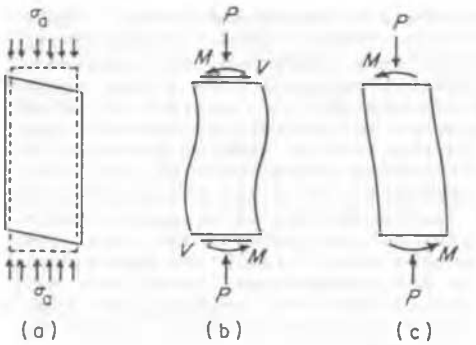

Figure 12. Exaggerated deformation of inclined specimen of anisotropic soil tested in the triaxial apparatus: (a) uniform state of stress; (b) end platens are horizontal, rough and rigid; (c) displacement when end platens are horizontal, smooth and rigid (after Saada and Bianchini, 1977).

of triaxial samples was noted by Saada and Bianchini (1977) - boundary measurements may be completely invalidated not only if the sample is misaligned but also if the axes of the test apparatus do not correspond with the axes of initial anisotropy of a correctly aligned sample (Fig. 12). An advantage of sticking to simple traditional test techniques and equipment is that testing can proceed without the operator being aware of the possibility that anything curious may be happening inside the apparatus. It is very easy to assume that effects that you choose not to look for do not exist.

Localisation of deformation within test specimens is also often tacitly ignored and can arise from the intrinsic character of the stress-strain response of the soil being tested without requiring defective experimental technique, although that may exacerbate the situation. Inhomogeneities within simple shear samples are well known (Airey et al, 1985) - but the boundary stress conditions in that apparatus are far from uniform even though the boundary displacements seem to be well controlled. Rigid boundary true triaxial devices of the Hambly (1969) type might be expected to force uniform deformations at all times but Desrues et al (1985) show convincing evidence that inhomogeneities are nevertheless able to develop.

In such an enclosed apparatus it is not possible to observe the progress of development of internal deformations but in plane strain tests this can be achieved by radiographic (Vardoulakis, 1988) or photogrammetric (Desrues and Hammad, 1989) techniques. Fig. 13, from a test on dense Hostun sand reported by Desrues et al (1985), is particularly interesting because it shows the development of major internal localisations of incremental deformation at a stage (3-4) immediately before the peak is observed in the stress-strain curve. The peak then emerges as a consequence of the development of this localisation and is not an intrinsic property of the soil. Continued monitoring of the internal deformation shows that the material in the region of localisation soon reaches a critical state and ceases to dilate further -

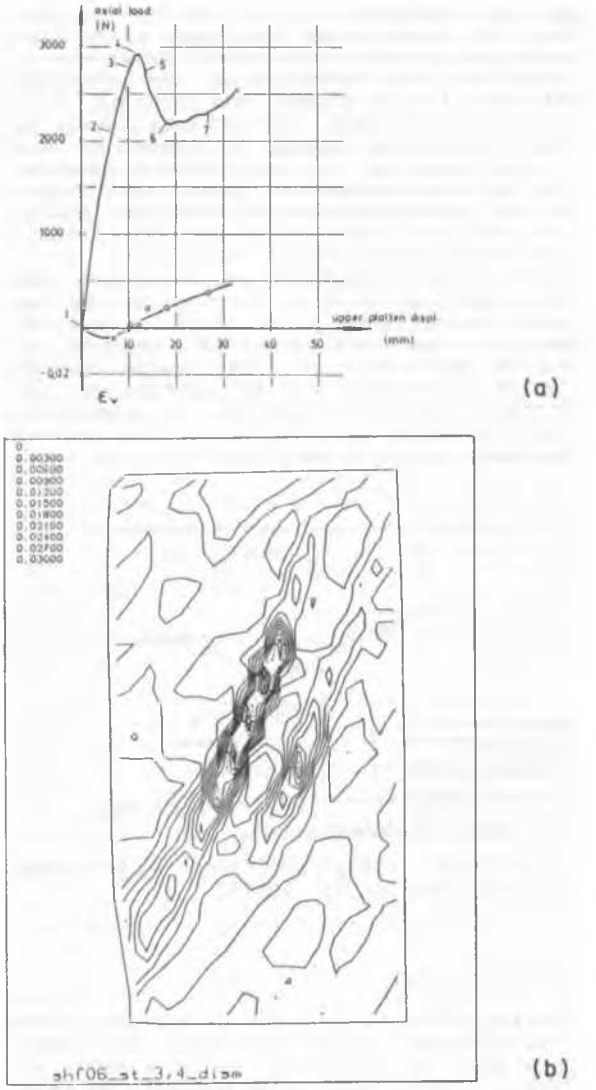

Figure 13. Localisation of deformation in plane strain test: Contours of shear strain for section 3-4 (from Desrues et al, 1985).

but this is not an observation that could be easily made on the basis of external measurements which are reflecting only the smeared average response of an extremely non-uniform sample.

Membrane penetration produces errors in volumetric strain measurement in triaxial tests on coarse grained soils - and consequently can lead to errors in stress path in undrained triaxial tests where the condition of no drainage merely preserves a constant mass of material upstream of the drainage valve and cannot actually preserve a constant volume of material. Lade and Hernandez (1977) performed experiments to show that membrane penetration could reduce the rate of increase of pore pressure in tests intended to study liquefaction of sand - and hence that conventional test methods might produce unconservative assessments of liquefaction potential. If it is an overall

picture of response that is requried - for example, the location of the steady state ine in terms of void ratio and effective stress - then provided the magnitude of the membrane penetration effect is known, the apparent void ratios can be corrected, and the maintenance of a strictly constant volume condition is not vital. The magnitude of the membrane penetration can be estimated either theoretically from assumptions about membrane thickness and stiffness and mean pore size (Baldi and Nova, 1984), or from direct experimental measurement in a series of calibration tests to determine the membrane penetration as a function of radial effective stress (Seed et al, 1989). Seed et al then use a computer controlled process to inject water to counter this calibrated membrane penetration - and show that the picture of the steady-state response of the sand is consistent with that obtained by allowing for the actual volume change in a standard test (Fig. 14).

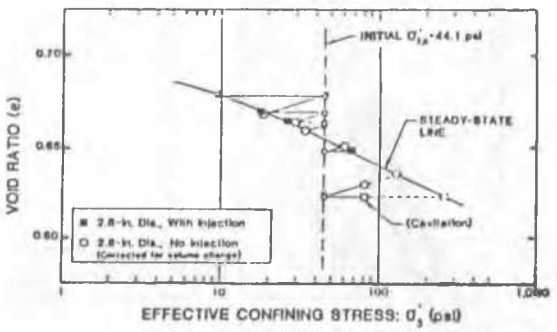

Figure 14. Steady state conditions for Monterey 16 sand (from Seed et al, 1989).

4.2 Effects of time

Much testing of soils proceeds on the assumption that time effects - other than those associated with movement of pore water as a result of gradients of excess pore water pressure - have no influence on soil behaviour. It is certainly important to be able to distinguish clearly between what may be called consolidation effects, which result only from the finite permeability of soils combined with the effective stress controlled soil response, and viscous effects. Viscous properties will lead to different observations of stress-strain response depending on the rate at which a test proceeds, will lead to creep under constant effective stress - the phenomenon known as secondary consolidation is an example of this - and will lead to relaxation of effective stresses if the soil is prevented from deforming. Some soils may show negligible viscous contribution to response but for many soils the possibility of viscous effects needs to be borne in mind in planning any laboratory test programme and in extrapolating laboratory test results to field conditions (Leroueil, et al, 1985a).

The correct interpretation of viscous effects in soils has to some extent become bogged down in the historic separation of primary and secondary consolidation: does creep occur during primary consolidation (Mesri and Feng, 1986; Leroueil et al, 1986)? The constitutive modellers have already overtaken this impasse - from a constitutive point of view it is clear that viscous effects must be associated with effective stresses and must be proceeding the whole time. Leroueil et al (1985b) describe a stress: strain: strain rate relation for one-dimensional compression of clays which provides this rational incorporation of viscous properties. This approach is generalised by, for for example, Adachi et al (1987) and more data in support of the presence of creep at all stages of consolidation are reported by Imai (1989) confirming the isotache model used by Leroueil et al (Fig. 15).

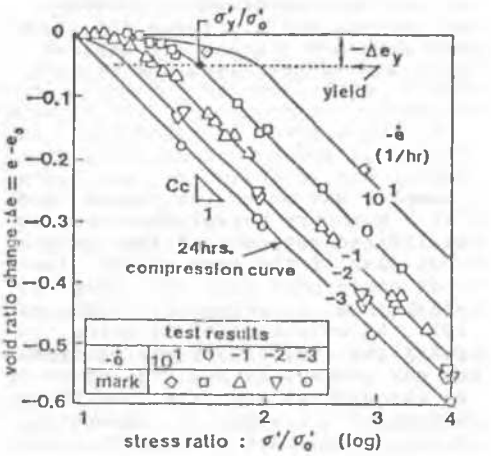

Figure 15. Isotaches for Yokohama Bay mud (from Imai, 1989).

4.3 Image analysis

Soils are assemblies of individual particles and although it is convenient to study soil behaviour in terms of the continum quantities of stress and strain the observed stress:strain response is merely the result of changes in interactions at the particulate level. Computer simulations (for example, Cundall, 1988) have been used to study the response of artificial assemblies of particles with appropriate descriptions of the contact mechanics, and to suggest micromechanical explanations for observed macroscopic mechanisms of response (Matsuoka et al, 1989). Experimental validation of these computer simulations has been achieved using arrays of two-dimensional elliptical photoelastic discs (Oda et al, 1985) from which both contact force and particle orientation information can be extracted. Other work has looked at particle orientations in, for example, resin impregnated sands but there has been little work on characterisation of the microstructure of clays and the linking of this microstructure with the mechanical history of the clay.

Electron micrographs provide direct visual indications of the microstructure of clays. From these, image analysis techniques can be used to automate - and make objective - the process of

extracting information about orientations of particles. Some preliminary results of observations on laboratory prepared samples of speswhite kaolin are reported by Smart and Tovey (1988). Rosette diagrams of particle orientations can be fitted approximately by ellipses (Fig. 16a) and the ratio of major to minor axes used to define an index of anisotropy I_a which is found to increase with the applied stress in one-dimensional compression (Fig. 16b). This work is continuing to look at the changes in quantitative fabric associated with different stress histories applied in a triaxial apparatus.

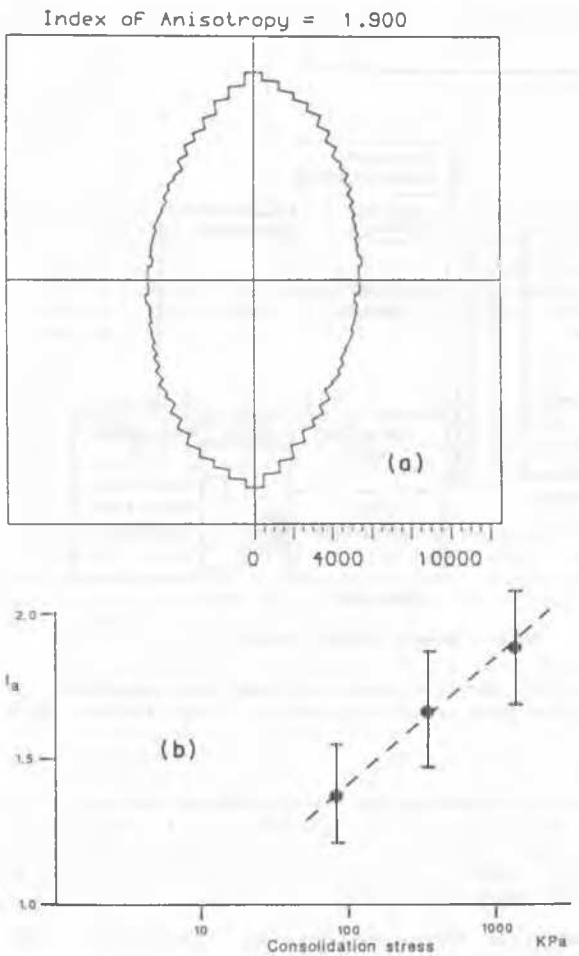

Figure 16. Development of anisotropy in speswhite kaolin: (a) Rosette diagram showing distribution of orientation in sample consolidated to 1360 kPa, (b) variation of anisotropy index with consolidation stress. (from Smart and Tovey, 1988).

Engineering classification of sands is generally based on particle size distribution & relative density, I_D, without much regard to particle morphology. For example two sands at the same relative density and having similar gradation curves may have widely different values of maximum & minimum specific volume, v (Burmister, 1962; Youd, 1973). Thus the maximum volume change potential of a sand (related to liquefaction potential under undrained cyclic loading) at a given effective confining stress will be significantly governed by the shape & angularity of sand grains (Ishihara & Watanabe, 1976; Castro, 1969; Vaid & Chern, 1985). Effect of particle angularity, gradation, and mineralogy on mechanical properties of sands has been investigated by Koerner (1968), Holubec & D'Appolonia (1973), Winterkorn & Fang (1975), Kapoor (1985), Clayton et al (1985), Yudhbir & Rahim (1987) and Rahim (1989).

While the importance of grain shape on mechanical behaviour of sands is now well recognised (NRC, 1985), methods to characterize particle shape quantitatively have not been standardized because of the tedious task of making numerous readings on small sized particles with which geotechnical engineer deals. However, a standard procedure to quantify particle shape would enable effective correlations between mechanical properties and particle shape index. The sedimentologists generally express shape interms of surface texture, roundness (angularity), and sphericity of grains (Blatt et el, 1971). Most commonly used index for particle roundness is the one due to Powers (1953) (Table 2). Also given in Table 2 is the description for each grade - term as recommended by Youd (1973).

Particle shape clearly differentiated from particle roundness (Wadell, 1932) is defined in terms of particle sphericity, ψ , expressed in terms of three dimensions of a particle - the longest dimension, d_L , the intermediate dimension, d_I, and the shortest dimension, d_S (Krumbein,1941). In addition to particle roundness and sphericity, Shape factor - defined in terms of flatness ratio $p = d_S / d_I$ and elongation ratio $q = d_I/d_L$ (Zingg, 1935; Lees, 1964) is also needed to fully define shape of a particle (Blatt et al, 1971).

Rahim (1989) developed a procedure for particle shape analysis in terms of form, angularity (roundness), sphericity, and shape factor using an Image Analyzer commonly employed by metallurgists for the study of surface characteristics of powders. An Image Analyzer, BOUSCH & Lamb make, Omnican Alpha 500, is a versatile system capable of providing full field measurements or measurements of individual feature in addition to tangent and intercept counts. The system consists of two major assemblies-microscope with a scanner, and a rack of basic, display, control and measurement modules (Fig. 17).

For the quantification of particle sphericity and shape factor, the following relationships were employed:

$$\psi = \sqrt[3]{\frac{d_S \cdot d_I}{d_L^2}} \qquad (1)$$

$$SF = \sqrt{\frac{d_S}{d_L \cdot d_I}} \qquad (2)$$

Procedure outlined by Griffiths (1967) was followed to avoid any ambiguity in the measurements of d_L, d_I, and d_S. The count mode of the image analyzer was used to determine the tan-

Table 2. Powers' roundness citeria & values

Roundness Class	Description	Roundness Interval	Mean Roundness
Very angular	Particles with unworn fractured surfaces and multiple sharp corners and edges	0.12-0.17	0.14
Angular	Particles with sharp corners and approximately prismoidal or tetrahedral shapes	0.17-0.25	0.21
Subangular	Particles with distinct but blunted or slightly rounded corners and edges	0.25-0.35	0.30
Rounded	Irregularly shaped rounded particles with no distinct corners or edges	0.49-0.70	0.59
Well Rounded	Smooth nearly spherical or ellipsoidal particles	0.70-1.00	0.84

gent count-taken as a measure of the number of protrusions along the boundary of the projected image of the particle (For details of Image Analyzer & procedures, see Rahim, 1989). The tangent count was carried out by examining 25-30 grains of each sieve fraction of a sand using the single feature count mode of the Image Analyzer, and the distribution of tangent count for each size fraction was evaluated. Average value of number of tangents, T, for a given sand was computed by the procedure used by Youd (1973) for calculating Powers' roundness index R. Average value of tangent count, T, was used to directly compare sands in terms of their angularity.

Distributions of average tangent count, T, for a variety of sands are depicted in Figs. 18 & 19. It will be readily seen that rounded to subrounded, subrounded to subangular, subangular to angular, and very angular sands have distinct tangent count patterns. Such distribution patterns may be used to classify sands on the basis of grain angularity. For the sands depicted in Figs. 18 & 19, Powers' roundness index, R, was also determdined as per the procedure adopted by Youd (1973). Fig. 20a shows an excellent inverse (as expected) relationship beween average T & R values. The following equation fits the data:

$$R = 0.14 \exp(2.7-0.225\ T) \qquad (3)$$

In this study T = 4 was taken to represent a well rounded grain. Equation (3) may be used to calculate R more systematically on the basis of T values rather than a subjective evaluation from Table 2 on the basis of purely visual comparisions between the actual particles and the standard shape classes.

Similar to Powers'index, R, coefficient of angularity, E - defined as the ratio of the measured specific surface of the sand particles to the specific surface of equivalent spheres (Hoffman, 1939) can also be used to quantify angularity of sands. Image Analyzer study provides data for computation of E values and the following relationships between E:R & E:T for the sands investigated are obtained:

$$R = 0.14 \exp(3.35-1.38\ E) \qquad (4)$$

$$E = 0.144\ (T + 4.83) \qquad (5)$$

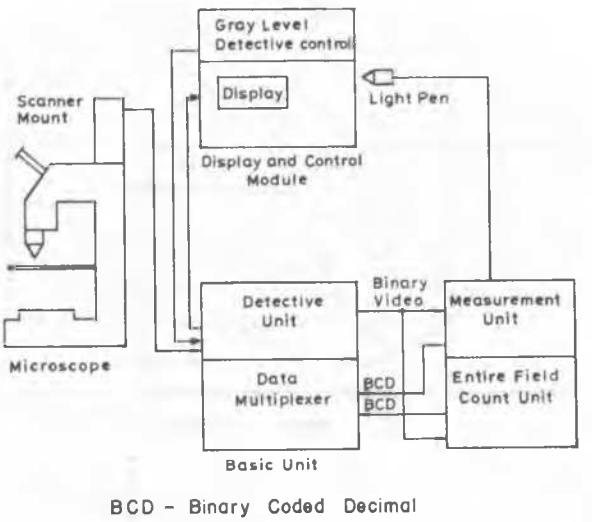

Figure 17. Block diagram of the Omnicon Alpha Image Analyzer with Microscope (from Rahim, 1989).

Holubec & D'Appolonia (1973) used E to quantify sand angularity. On the basis of available data the value of E varies from 1.24 for rounded sands (R = 1.0) to 2.54 for very angular sands (R = .12).

The particle shape analysis was carried out in terms of sphericity ψ & shape factor, SF. Fig. 20b shows a relationship between ψ & SF on the basis of which the following shape subdivisions may be made.

Flaky oblate grains $\psi \leq 0.64$

Bulky elongated grains $0.64 < \psi \leq 0.74$

Bulky elipsoidal grains $\psi > 0.74$

Following relationship between SF & ψ is suggested:

$$SF = 1.538\ \psi - 0.48 \qquad (6)$$

For a more detailed particle shape analysis

Table 3. Characterization of sands.

Sand	Gradation		Volume Change Potential		Morphology					Mineral** %	Physical Description
	C_U	d_{50} mm	V_{max}	V_{min}	ψ	SF	R	E	T		
Standard	1.39	0.475	1.81	1.49	0.81	0.77	0.79	1.27	4	Q=98-100 F=0-2	Bulky, Spheroidal, rounded to well rounded grains
Calcareous	1.78	0.43	2.05	1.57	0.67	0.55	0.55	1.49	6	Q=5 C=95	Flaky, Oblate, angular grains composed of shells
Ganga	2.57	0.18	2.25	1.577	0.68	0.54	0.19	2.32	11	Q=60-65 F=20-25 M=8-10 C=2-3	Flaky, Oblate, Angular Grains
Kalpi*	4.81	1.0	1.91	1.48	0.70	0.60	0.14	2.42	12	Q=40 F=40 M=1-2 C=18	Bulky, elongated Very angular grains Coated with Carbonate

** Q - Quartz, F - Feldspar, M - Mica, C - Carbonate (Calcite, Aragonite)

* Kalpi is not a typical river sand like Ganga since its distance of transport from source is very short and the grains are coated with Carbonate deposited by the percolating ground water. These special characteristics are responsible for its typical tangent count distribution.

Zingg diagram is recommended. Typical results for Ganga sand (see Table 3) are shown in Fig. 21. Distribution of particles with different shapes is well illustrated in the Zingg diagram.

Based on shape & roundness studies carried out by Rahim (1989), a variety of sands have been characterized (Table 3). It is recommended that a sand may now be more fully characterized on the basis of the following:

(i) Morphological characteristics defined in terms of R (computed from T count), ψ and SF.
(ii) Mineralogical composition.
(iii) Gradational characteristics in terms of indices such as C_U, d_{50}
(iv) Volume change potential parameters: v_{max} v_{min}.

Of the indices ψ, SF, R & E, the values of ψ & SF for widely different sands lie in a narrow range where as the values of R practically cover the entire range (0-1.0); same is true in case of E & T values. Holubec & D'Appolonia (1973) used index E to correlate axial strain & angle of shearing resistance, ϕ', (at a given normal stress & relative density) for different sands. Rahim (1989) has successfully correlated roundness index R (computed from T values) with the coefficients m_o, m_1, m_2 & c_o, c_1, c_2 in the following two relationships for sands (also see Bellotti, et al, 1985):

$$M = m_o (\sigma')^{m_1} \exp(m_2 I_D) \quad (7)$$

$$q_c = c_o (\sigma')^{c_1} \exp(c_2 I_D) \quad (8)$$

where M is constrained modulus, q_c is static cone resistance, & σ' is effective confining stress.

These investigations would suggest the desirability of adopting Image analyzer as a useful tool for quantification of shape and angularity of sands. In addition to providing quantitative indices such as ψ, SF, and R, the use of Image Analyzer would provide a physical appreciation of the nature of the material to the investigator. It may also be desirable to standardize the suggested procedure of measuring number of tangents, particle dimensions, and projected surface area so that determination of ψ, SF, E and R (from tangent count T) can be made part of the process of characterization of sands.

5. DEVELOPMENTS IN INTERPRETATION

5.1 Presentation of experimental results

Test data should be presented in such a way as to provide the maximum of information to the viewer, with the maximum of objectivity, and the minimum of laundering between test apparatus and published charts. In many ways the optimum way of disseminating test data to constitutive modellers is in the form of tables of stresses and deformations, available on microcomputer diskettes, in which basic apparatus corrections have been applied (for membrane restraint, apparatus compliance, etc) but which contain absolutely no subjective interpretation. As soon as it is required to display data for a more general reader, then bias can easily enter.

There is an advantage in exercising some care in selection of stress and strain quantities in terms of which data are to be presented. The use of properly work conjugate stress and strain quantities both preserves some element

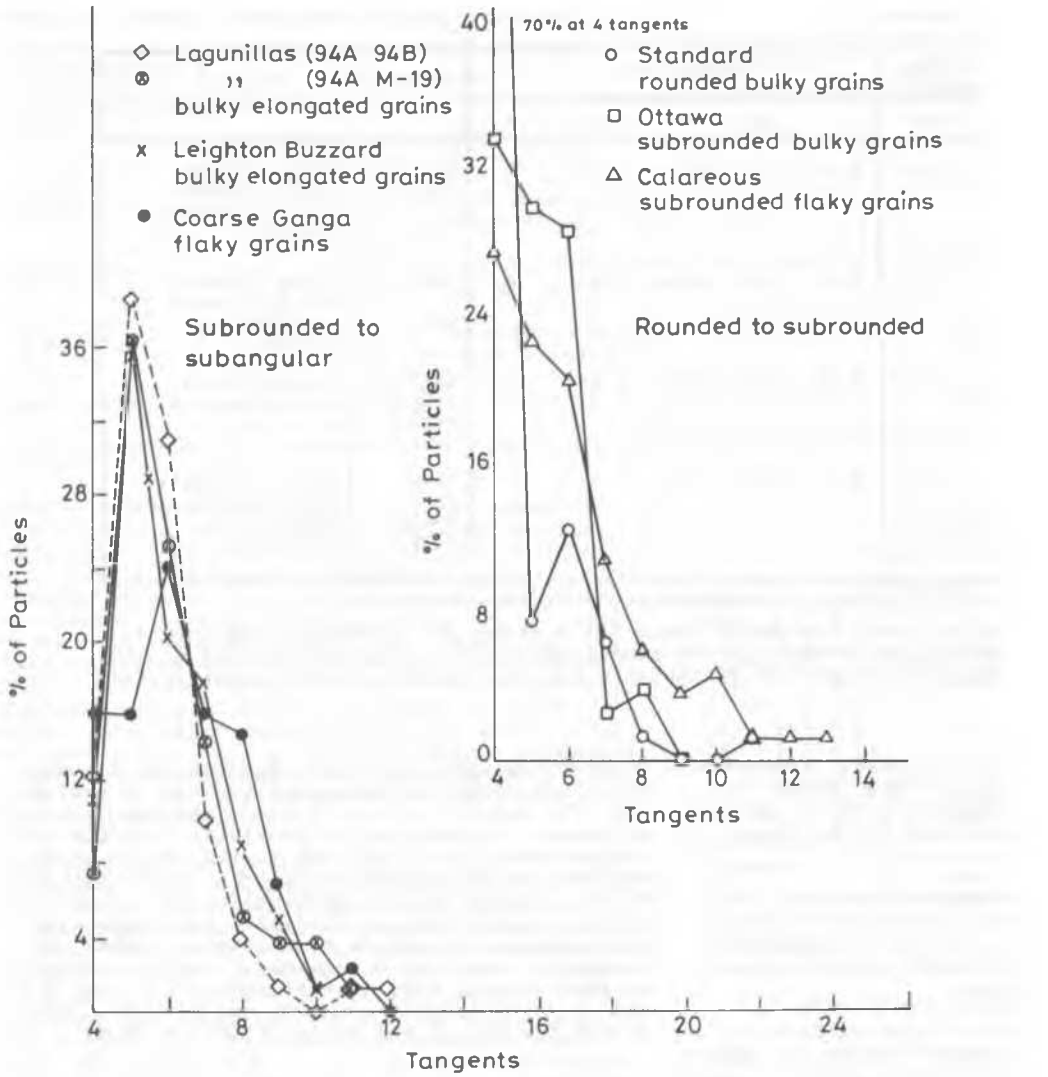

Figure 18. Typical distribution of grain irregularities (related to number of tangents measured with Image Analyser) for rounded to subrounded and subrounded to subangular sands (from Rahim, 1989).

of objectivity and is likely to be compatible with basic features of constitutive models which are trying to describe the data. Thus, development of Cambridge soil mdoels, such as modified Cam clay (Roscoe and Burland, 1968), always placed great emphasis on the importance of using appropriate stress and strain quantities for the description of triaxial test data. With axial effective stress σ_a' and radial effective stress σ_r' and corresponding strain increments $\delta\varepsilon_a$ and $\delta\varepsilon_r$, the stress quantities which can most usefully be used to identify different components of soil response are the mean stress,

$$p' = (\sigma_a' + 2\,\sigma_r')/3 \qquad (9)$$

and the work conjugate volumetric strain increment

$$d\varepsilon_p = d\varepsilon_a + 2\,d\varepsilon_r \qquad (10)$$

On the one hand, and the deviator stress,

$$q = \sigma_a' - \sigma_r' \qquad (11)$$

and its work conjugate triaxial shear strain increment

$$\delta\varepsilon_q = 2(\delta\varepsilon_a - \delta\varepsilon_r)/3 \qquad (12)$$

on the other. The increment of work is then compeltely given by

$$\delta W = p'\,\sigma\varepsilon_p + q\,\delta\varepsilon_q \qquad (13)$$

and volumetric and distortional effects have been separated. (The subscripts p and q on the strain variables indicate the stress quantity with which each is associated). An objective way of presenting test data is then to show effective stress paths in p':q space with vectors superimposed to show the direction and

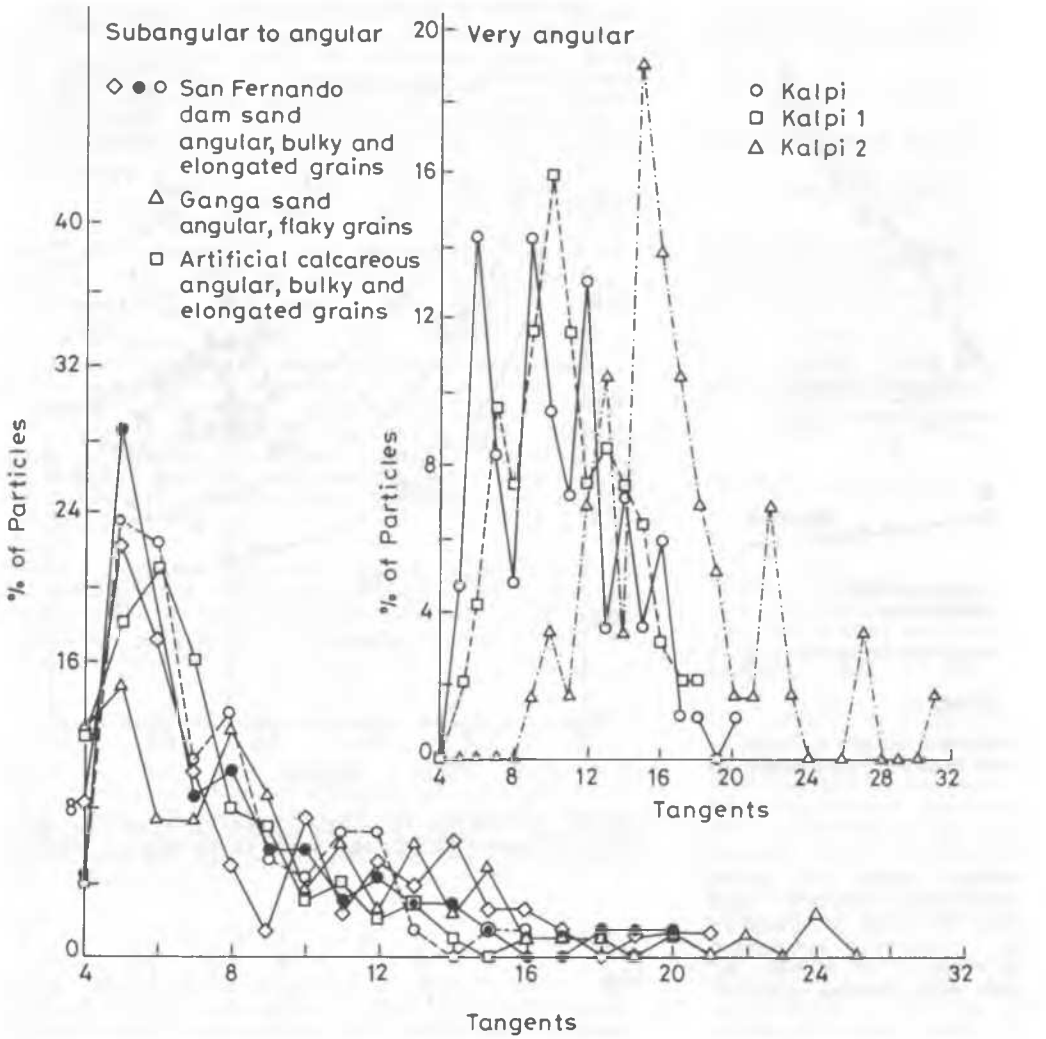

Figure 19. Typical distribution of grain irregularities (related to number of tangents measured with Image Analyzer) for subangular to angular and very angular sands (from Rahim, 1989).

magnitude of the strain increment $\delta\varepsilon_p : \delta\varepsilon_q$ at each point; and strain paths in $\varepsilon_p : \varepsilon_q$ space with vectors superimposed to show the direction and magnitude of the stress p':q at each point (Fig. 22). Of course, even this division into volumetric and distortional parts itself represents a subjective division concerning the way in which data should be interpreted.

So far as the development of constitutive models is concerned the widely used MIT stress variable $(\sigma_a' + \sigma_r')/2$ is a definite hindrance in presenting triaxial test data because it is not a proper volumetric stress quantity.

For true triaxial tests, in which no rotations of principal axes occur, a separation into volumetric and distortional effects can be achieved by using the mean stress

$$p' = (\sigma_1' + \sigma_2' + \sigma_3')/3 \qquad (14)$$

and the volumetric strain increment

$$\delta\varepsilon_p = \delta\varepsilon_1 + \delta\varepsilon_2 + \delta\varepsilon_3 \qquad (15)$$

on the one hand, and the stress deviators

$$\sigma_1' - p';\ \sigma_2' - p';\ \sigma_3' - p'$$

and corresponding strain deviators

$$\delta\varepsilon_1 - \delta\varepsilon_p/3;\ \delta\varepsilon_2 - \delta\varepsilon_p/3;\ \delta\varepsilon_3 - \delta\varepsilon_p/3$$

On the other. The deviatroic information can then be displayed in π-plane views of principal stress space and principal strain space, since the sum of each set of deviatoric quantities is zero. Once again, vectors of strain increments can be superimposed on the stress path, and vectors of stresses can be superimposed on the strain path (Fig. 23).

Where rotations of principal axes occur, in the simple shear apparatus, hollow cylinder apparatus, and directional shear cell, then presentation in terms of principal stresses conceals

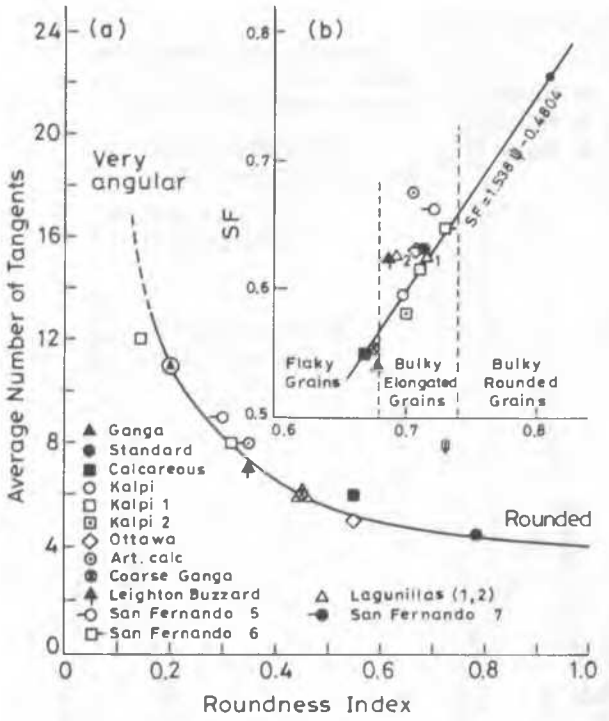

Figure 20. Relationship between tangent count (related to angularity) and Powers roundness index (from Rahim, 1989).

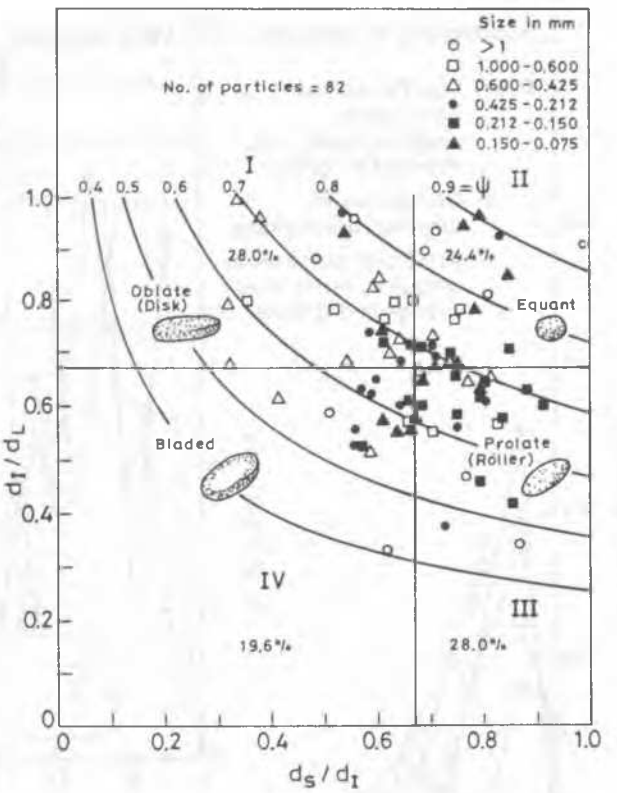

Figure 21. Particle shape classification using Zingg diagram for Ganga sand (from Rahim, 1989).

information, since principal axes of both strain increment and stress will rotate, and there is no need for these two sets of principal axes to be coincident. The work increment can then not be written simply in terms of principal strain increment and stress quantities.

Where rotation of principal axes occurs under conditions of plane strain, so that $\varepsilon_y = 0$ and the corresponding dependent stress σ_y' is a principal stress, then useful pairs of stress and strain quantities are the mean stress in the plane of shearing

$$s' = (\sigma_z' + \sigma_x')/2 \qquad (16)$$

and the volumetric strain increment

$$\delta\varepsilon_s = \varepsilon_z + \varepsilon_x \qquad (17)$$

a stress difference quantity

$$\beta = (\sigma_z' - \sigma_x')/2 \qquad (18)$$

and a corresponding strain difference quantity

$$\delta\zeta = \delta\varepsilon_z - \delta\varepsilon_x \qquad (19)$$

and the shear stress τ_{zx} and shear strain increment $\delta\gamma_{zx}$ in the plane of shearing. The increment of work is then

$$\delta W = s'\,\delta\varepsilon_s + \beta\,\delta\zeta + \tau_{zx}\,\delta\gamma_{zx} \qquad (20)$$

These will be relevant to the simple shear apparatus and the directional shear cell.

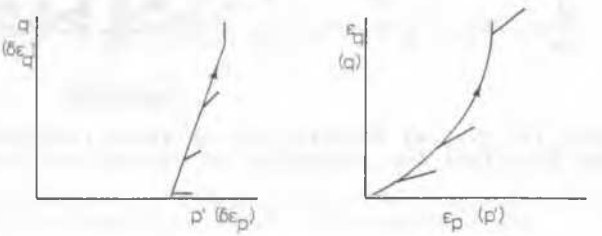

Figure 22. Presentation of triaxial test results.

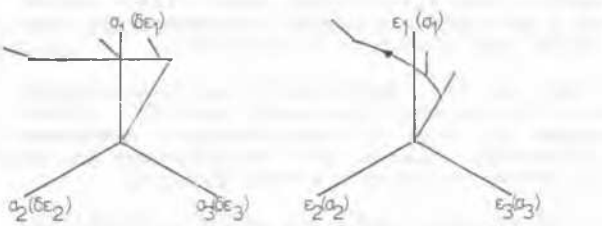

Figure 23. Presentation of deviatoric true triaxial results.

Rotations of principal axes are not useful variables for display of experimental data since they can not be grouped into work conjugate pairs. However, the stress and strain variables suggested here give direct indications of rotations of principal axes. The direction of the major principal stress Ψ is given by

$$\tan 2\Psi = \tau_{zx}/\beta \qquad (21)$$

and the direction of the major principal strain increment ξ is given correspondingly by

$$\tan 2\xi = \delta\gamma_{zx}/\delta\zeta \qquad (22)$$

The length of the stress vector directly indicates the magnitude of the quantity $(\sigma_1' - \sigma_3')/2$, that is, half the difference between the principal stresses in the plane of shearing. Similar statements can be made about the lengths of the stress increment and strain increment vectors.

Wood, Drescher and Budhu (1979) show that for many simple shear tests on sand (and possibly also some on normally consolidated clay) the rotations of principal axes are controlled by the expression

$$\tau_{zx}/\sigma'_z = k \tan \Psi \qquad (23)$$

where k is a soil constant linked with the critical state characteristics of the soil. It can then be shown that in a typical simple shear test performed with constant vertical effective stress σ_z' the path in the β:τ_{zx} plane is a parabola:

$$2k\beta\, \sigma_z' = k^2\, \sigma_z'^2 - \tau_{zx}^2 \qquad (24)$$

Such a curve is sketched in Fig. 24: this method of presenting the simple shear stress:strain data makes the deviation between the directions of the principal stress, the principal stress increment, and the principal strain increment apparent.

In the simple shear apparatus the strain in the x direction is always zero so that the vertical strain $\delta\varepsilon_z$ is the same as both the volumetric strain and the new strain increment variable $\delta\zeta$. The direction of the strain increment vector $\delta\zeta$: $\delta\gamma_{zx}$ then additionally gives a direct indication of the rate of dilation that is occurring.

The principal stress σ_y' in the lateral direction of zero strain will not be constant during a simple shear test - to study the variation of σ_y' a further plotting plane is needed.

In the hollow cylinder apparatus there are in principle four degrees of freedom since the sample is not forced to maintain a condition of plane strain. Thus the strain $\delta\varepsilon_y$ will not be zero even though the corresponding stress σ_y' will still be a principal stress. The choice of work conjugate pairs of stress and strain quantities is now less clear cut. Because volume changes are so important in soils it may still be desirable to separate volumetric and distortional effects. Then a suitable set of stress and strain variables might be mean effective stress

$$p' = (\sigma_1' + \sigma_2' + \sigma_3')/3 = (\sigma_x' + \sigma_y' + \sigma_z')/3 \qquad (25)$$

and volumetric strain increment

$$\delta\varepsilon_p = \delta\varepsilon_1 + \delta\varepsilon_2 + \delta\varepsilon_3 = \delta\varepsilon_x + \delta\varepsilon_y + \delta\varepsilon_z; \qquad (26)$$

the stress variables β and τ_{zx}, and strain increments $\delta\zeta$ and $\delta\gamma_{zx}$ as before; and a deviator stress for the y direction

$$\eta = \sigma_y' - p' \qquad (27)$$

and corresponding deviator strain increment

$$\delta\mu = 3(\delta\varepsilon_y - \delta\varepsilon_p/3)/2. \qquad (28)$$

The work increment is then

$$\delta W = p'\, \delta\varepsilon_p + \beta\, \delta\zeta + \eta\, \delta\mu + \tau_{zx}\, \delta\gamma_{zx}. \qquad (29)$$

Though the definition of $\delta\mu$ is awkward, most of the action in hollow cylinder tests occurs in the zx plane, and rotations of principal axes will be correctly shown in a diagram such as Fig. 24.

The hollow cylinder tests reported by Shibuya and Hight (1989) and Sayao and Vaid (1989) were performed with constant principal stresses so that the paths followed were arcs of circles in the β:τ_{zx} plane. (whereas in simple shear tests the intermediate principal stress σ_y' changes because the corresponding strain is fixed at zero, in these hollow cyulinder tests the intermediate principal stress σ_2' is kept constant and the corresponding strains will vary).

The advantage of this mode of presenting test results may appear negligible when it is only the results of rather ordinary simple shear or hollow cylinder tests that are being considered. However, it comes into its own when the results of probing tests in the directional shear cell such as those described by Sture et al (1988) are studied. In this programme of tests stress space was probed both in a cubical cell (true triaxial apparatus) and in the directional shear cell. The directional shear cell was treated merely as a device allowing further freedom to explore general stress space : the tests were specified as rosettes of straight stress paths in the β : τ_{zx} plane to be applied to a series of samples with the same stress history. On any one of the stress probes both the direction of the principal axes of stress and the magnitudes of the principal stresses in the plane of shearing changed continuously. A typical experimental result is shown in Fig. 25. The basic philosophy behind this sort of testing is that soil behaviour will be reasonably continuous on continuous stress paths with no sudden major changes in stiffness expected to be associated with passage of the stress path through the axes of the β : τ_{zx} plane (for principcal stress directions of 0°, 45°, 90° etc). In this respect the results reported by Sayao and Vaid (1989) seem curious with marked discontinuity of strain development as the direction of the principal stress passes through the vertical.

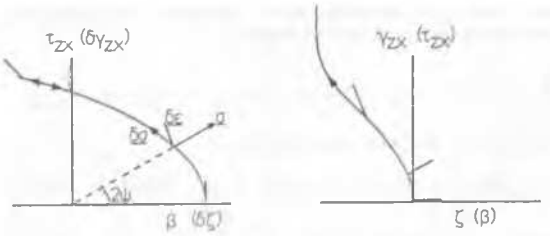

Figure 24. Presentation of results of plane tests with rotation of principal axes.

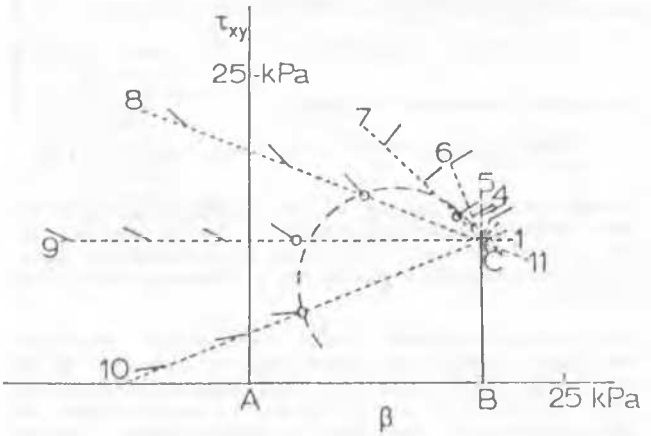

Figure 25. Directional shear cell tests on Leighton Buzzard sand: series of stress probes for samples with history ABC (data from Sture et al, 1988).

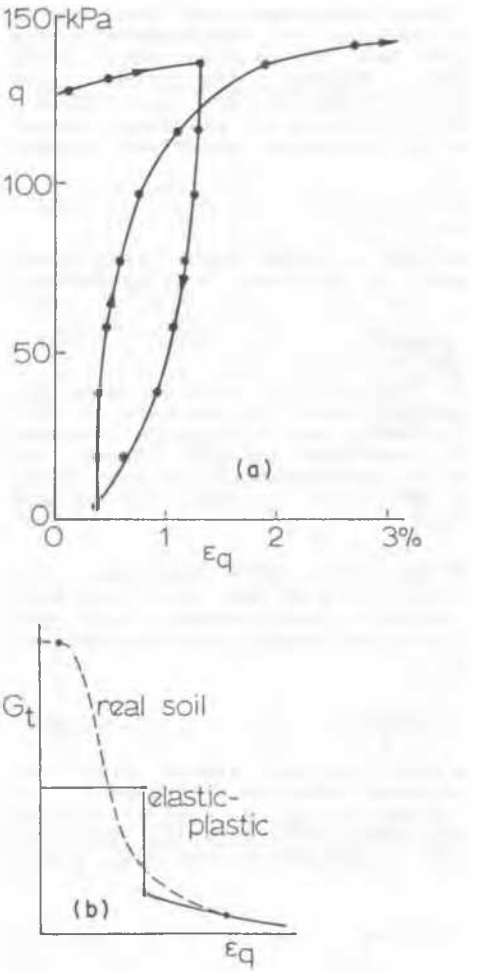

Figure 26. Spestone kaolin: (a) cycle of undrained loading; (b) variation of stiffness with strain (after Roscoe and Burland, 1968).

5.2 On the yielding of soils

The phrase "yielding of soils" used by Roscoe et al (1958) partly describes pre-failure behaviour in a rather general way and in particular is associated with the idea of a state boundary surface limiting attainable states of effective stress and volumetric packing - a feature that is part also of numerical models for soil such as modified Cam clay (Roscoe and Burland, 1968). The term "yielding' is now probably more correctly associated with the transition from elastic to plastic soil response, which is to say, with the onset of irrecoverable deformations. Elastic-plastic models, of which modified Cam clay is but one rather simple example, introduce yield surfaces bounding regions in stress space which can be explored without any irrecoverable deformations being incurred.

If yield surfaces are to be a fundamental element in soil models then it is necessary that experimental studies should at least provide some evidence of their existence. This is not often done, primarily because the testing required to discover the full details of shape and size of a yield surface for a soil with a given history would be beyond the scope of most test programes. As a result models are usually fitted to experimental data simply by optimising the parameters of the model which is several steps removed from the verification of the hypotheses of the model.

If a serious attempt were made to discover the extent of the truly elastic region for a soil - the region in which all work done in deforming the soil element was converted to stored strain energy that could be completely recovered - then it would probably be concluded that no such elastic region actually exists. Practically, of course, the typical unloading-reloading response of a soil (Fig. 26a) can be idealised as elastic-plastic but the simplification of the hysteretic unload-reload loop into reversible elasticity has clearly lost a lot of information concerning the real soil behaviour.
In terms of tangent stiffnesses, the relationship between incremental stresses and strain, the assumed variation of stiffness with strain is shown by the solid line in Fig. 26b: when the yield strain is reached then the tangent stiffness drops sharply from its initial, high elastic value. The actual experimentally ob-

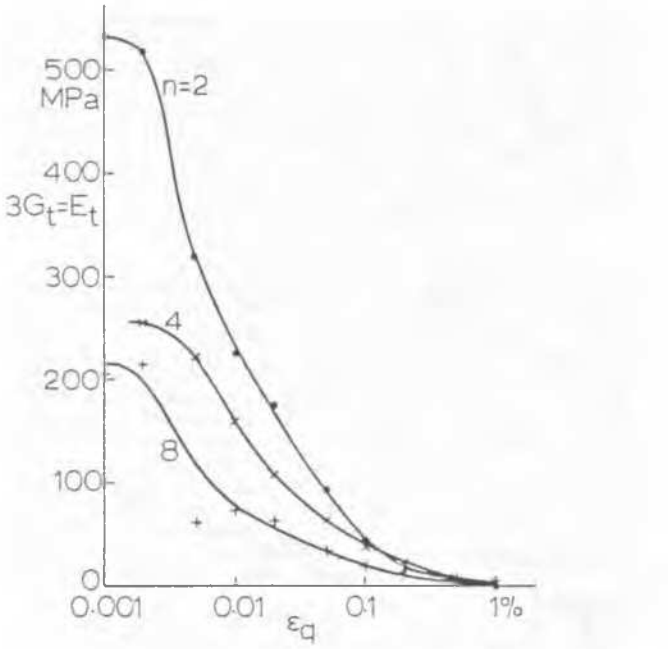

Figure 27. Variation of stiffness with strain in undrained compression of one-dimensionally over-consolidated North sea clay (data from Jardine et al, 1984).

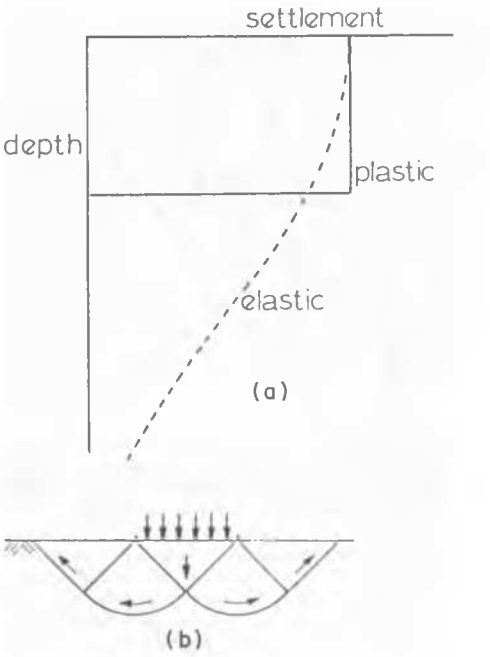

Figure 28. Profiles of settlement beneath footing.

served response corresponds to the dotted curve in Fig. 27. Whether the distinction between idealisation and reality actually matters depends on the use to which the idealised model is going to be put. If the loading of a geotechnical structure takes most significant soil elements into regions of stress space that the model regards as plastic, with corresponding low tangent stiffness, then it may not matter too much how the low strain stiffness is described in detail. However, if the loading only produces stress changes that the model regards as elastic then correct description of this low strain response will be crucial.

Out of the work of Jardine et al (1984) has emerged an understanding that even stiff soils that would conventionally be considered as elastic show significant variations of stiffness with strain in a region that a model such as modified Cam clay would describe as elastic. Old habits die hard and it is still common to find stiffness variations plotted as variations of secant modulus with strain. This unfortunately merely serves to perpetuate the fiction that this is an elastic process that is being observed - the fact that hysteretic dissipation of energy occurs on virtually all cycles of unloading and reloading of soils (Fig. 26a) should dispel that particular fiction.

Secant shear stiffness G_s and tangent shear stiffness G_t can be related. For example, in undrained triaxial tests:

$$G_s = q/3\varepsilon_q \qquad (30)$$

$$G_t = dq/3d\varepsilon_q = G_s + dG_s/d\varepsilon_q \qquad (31)$$

and this serves to demonstrate that tangent or incremental stiffness will fall much more rapidly than secant stiffness. Data reported by Jardine et al (1984) for a North Sea clay have been reinterpreted in terms of tangent stiffness in Fig. 27. It is clear that the drops in stiffness occur over a very small range of strain.

The consequences of this fall of stiffness with strains can be illustrated for an extreme case by considering the profile of settlement with depth beneath the centre of a strip footing on an elastic layer of soil (constant stiffness with strain - dotted line in Fig. 28a) and on a plastic soil (zero tangent stiffness - solid line in Fig. 28a). The elastic soil shows a pattern of deformation which extends to great depth. The plastic material localises the deformation near the surface in a plastic collapse mechanism (Fig. 28b). The effect of a smoothly varying stiffness with strain will be less extreme but will also lead to a much more localised pattern of deformation in the soil.

The distributions of displacement for elastic and plastic soils have been normalised to the same surface value in Fig. 28 and in general an equivalent elastic secant modulus could be chosen which would give the correct calculated displacement at one point around any geotechnical structure (Jardine et al, 1986). However, the pattern of displacements that an elastic analysis implies would be totally different from that actually obtaining in the soil and, if differential movements are of concern, or movements in the ground at a point away from the structure - such as the effect of an excavation on adjacent buildings or services - then correct modelling of the falling tangent stiffness of the soil will be imporant.

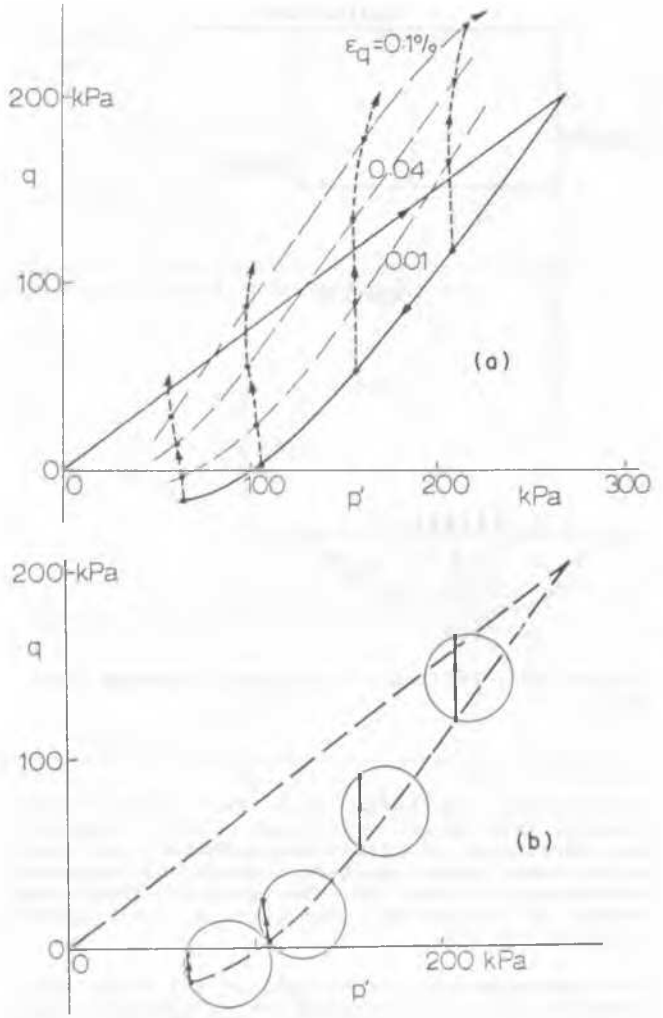

Figure 29. Undrained compression of one-dimensionally overconsolidated North sea clay: (a) contours of shear strain; (b) kinematic yield locus (after Jardine et al, 1984).

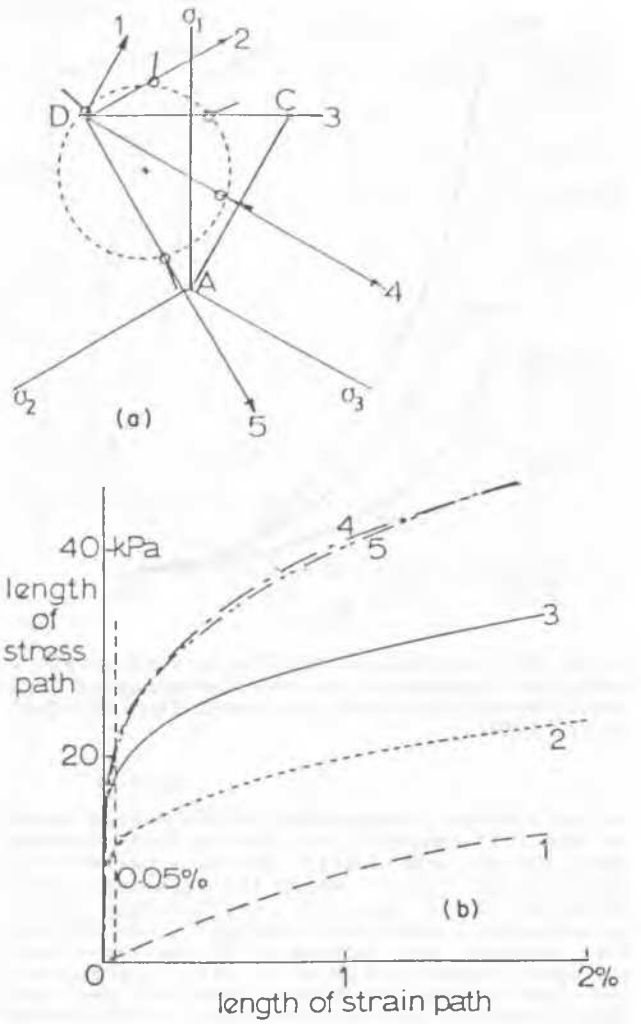

Figure 30. True triaxial stress probes on Leighton Buzzard sand with standard history ACD: (a) small strain offset contour (b) stress: strain relations (from Alawaji et al, 1987).

A general observation that can be made concerning stiffness of soils is that whenever a stress path or strain path contains a corner then the tangent stiffness of the soil will increase, but decrease as the stress state progresses along a smooth path away from that corner. Such an observatiodn can be made in true triaxial tests (Alawi, 1988), directional shear cell tests (Wong et al, 1987) and conventional triaxial tests (Jardine et al, 1984). Some of these latter triaxial test results, on a reconstituted North Sea clay, are shown in Fig. 29 both as presented by Jardine et al in terms of contours of shear strain for undrained loading following one-dimensional loading and varying degrees of unloading (Fig. 29a), and in terms of a small kinematic yield surface, bounding the region of stress space which can practically perhaps be treated as purely elastic (Fig. 29b) - corresponding to the "bubble" model described by Al-Tabbaa and Wood (1989).

Such a kinematic yield surface may be a convenient numerical approximation to a complex observed response but observation of sharp yield points in soil is unfortunately rare. It may be more acceptable to characterise the kinematic response in terms of a contour of a certain level of strain offfset as is frequently done in metal plasticity (see, for example, Ikegami, 1982). Thus Fig. 30 presents a contour of strain offset ε = 0.05% (where $\varepsilon^2 = 2[(\varepsilon_2 - \varepsilon_3)^2 + (\varepsilon_3 - \varepsilon_1)^2 + (\varepsilon_1 - \varepsilon_3)^2]/9$) for one set of true triaxial tests on dry Leighton Buzzard sand reported by Alawaji et al (1987). Each of five samples was subjected to the same purely deviatoric stress history ACD and then subjected to backward probes in each of the directions D_1, D_2, D_3, D_4 & D_5 (Fig. 30a). The resulting deviatoric stress:strain responses plotted simply as length of stress path from D against length of strain path from D are shown in Fig. 30b. Though it is clear that no sharp

yield phenomena can be observed, it is also clear that the strain offset ϵ = 0.05% does indicate a stage on each curve at which the stiffness is rapidly decreasing so that this strain offset contour in Fig. 30a gives some indication of the position of the current quasielastic region for this sand. Alawaji et al explore also the link between the location of the 0.05% strain offset contour and the stress and strain history of the soil.

With this background it does not seem to be possible to use parts of stress paths that are well away from corners to define the elastic properties of soils. This seems to throw some doubt on the experimental procedure proposed by Atkinson et al (1989). They observe that the stiffness matrix is symmetric (non-zero off-diagonal terms are interpreted as indicating anisotropic elasticity) and hence deduce that the soil is responding elastically, but an elastic-plastic soil obeying an associated flow rule would also show a symmetric matrix - and on the stress paths followed the "bubble" model of Al-Tabbaa and Wood (1989) would indeed suggest inelastic behaviour.

There is clearly an element of pragmatism to be borne in mind here in interpreting experimental data for subsequent use in calculating response of geotechnical structures. Elastic-plastic kinematic hardening models may be required if the paths followed during the sequence of construction of a geotechnical structure contain many corners. If the loading is essentially monotonic, however, then it may instead prove computationally advantageous to use a non-linear "elastic" model of the sort described by Yin et al (1989) (though this does actually include an elastic-plastic distinction). Conceptually it seems that an elastic-plastic model will provide a more rational and formal way of extrapolating from available laboratory test data: and one which is less likely to be restricted only to the regions of stress space from which the laboratory data were obtained.

5.3 Changes in sand gradation & particle shape during testing

Sands unlike clays undergo changes in grain shape, size, and gradation during compression and shear. The degree of alteration of grains depends upon mineralogy, particle size, angularity, and stress level. These changes are known to significantly alter the behaviour of sands in respect of compressibility and shearing resistance (for a detailed discussion see Rahim, 1989). Two distinctly different phenomena lead to sand particle degradation during compression and shear. They are:

(i) Grain modification at low stress levels when the grain boundary protrusions are knocked off without any grain splitting. This leads to significant reduction in grain angularity & also some changes in sand gradation.
(ii) Grain splitting (crushing) at very high stresses which would again produce angular grains with significantly different gradation.

While sufficient data on particle crushing under high stresses are available in literature (Hardin, 1985) very little information is reported on the degree of particle modification. It is well known that particle angularity and gradation significantldy control the maximum & minimum values of specific volume, and hence the specific volume range (v_{max}-v_{min}) of sands available at very low stress levels (Youd,1973). Also the compressibility of a sand and the peak angle of shearing resistance are known to be correlated to particle angularity size, and gradation (Holubec and D'Appolonia, 1973; Winterkorn & Fang, 1975; Clayton et al 1985; Yudhbir and Rahim, 1987). Given the strong influence of grain angularity, size, and gradation on the engineering behaviour of sands, the investigation of degree of grain modification during compression and shear assumes added importance.

Rahim (1989) has reported results of a detailed sutdy on grain crushing and modification during compression for a variety of sands. The potential for the grain degradation in terms of size, angularity, and shape alterations including crushing is best demonstrated through the study of changes in grain size distribution curves of a sand before and after loading. Hardin (1985) proposed the calculation of breakage potential, B_p , for particle degradation on the basis of the area of grain size gradation curve (Fig. 31a). B_p reflects the total potential for change of grain shape and size under stress for a given sand and includes both the potential modification & crushing. On the basis of all available data, Rahim (1989) has shown that B_p is uniquely related to the average particle size, d_{50}, as shown in Fig. 32.

In addition to index B_p, Hardin (1985) proposed an index B_T as a measure of particle breakage (Fig. 31b). Fig. 33 brings out the influence of particle angularity, mineralogy, d_{50}, relative density, and stress level on particle breakage index B_T. At the same stress level (8000 kN/m^2) samples of crushed granite (Lee & Farhoomand, 1967) with same C_U, grain mineralogy, and angularity show consistent increase in B_T with d_{50}. Well rounded quartz sands (Ottawa and Mol sands) show similar trends. Angular kalpi and Napa basalt samples also exhibit an increase in B_T with d_{50} but the rate of increase is greater compared to rounded & subrounded to subangular grains. For the same value of d_{50} and relative density, loose sample of Ganga sand shows B_T equal to 1.9 times that for Tayoura sand at the same stress level. This is primarily due to the fact that angular Ganga sand is micaceous (8-10 % mica) compared to the quartz-feldspar subrounded-subangular Tayoura sand. Effect of relative density on B_T is shown for loose (I_D = .24) and dense (I_D = 0.9) samples of Tayoura sand. For the same initial relative density (I_D = .24) B_T for Tayoura sand increases from .035 to .095 as the stresses increases from 17600 kN/m^2 to 45000 kN/m^2.

For the same mineralogy, d_{50}, and stress level B_T has also been shown to decrease with increasing C_U (Rahim, 1989). Rahim has also shown that for most natural sands particle crushing does not commence until a stress level of around 8000 kN/m^2.

Based on resutls available it may be suggested that, except for the case where aggregated

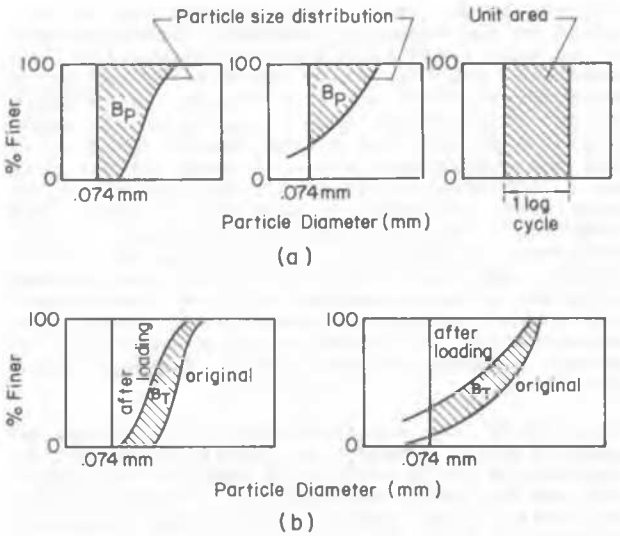

Figure 31. Definition of breakage potential (a) and total breakage (b) (from Hardin, 1985).

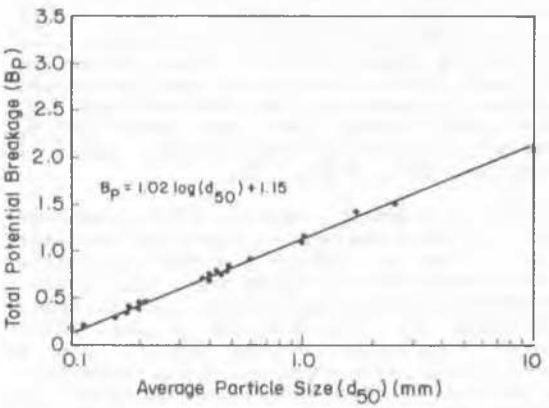

Figure 32. Relationship between total potential breakage, B_p, and average particle size, d_{50}. (from Rahim, 1989).

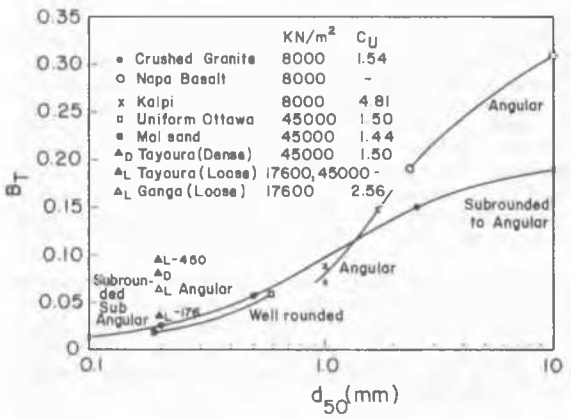

Figure 33. Factors governing total sand particle breakage, B_T (from Rahim, 1989).

grains are involved, both B_p & B_T for sands of similar gradation, angularity & mineralogy, increase with particle size (d_{50}) whereas relative breakage index $B_r = B_T / B_p$ (Hardin, 1985) at a given stress level remains essentially the same (Rahim 1989). Particle degradation of different sands can thus be best expressed in terms of the relative breakage index B_r. Rahim (1989) has shown an excellent correlation of B_r with mineral composition of a sand.

While data on grain crushing is relevant to the behaviour of different sands at elevated stress levels, grain modification studies are important to understand the behaviour of sands in the range of stresses commonly investigated in triaxial testing. Since loose samples would experience more grain modification compared to dense samples, Rahim (1989) investigated four sands at an initial relative density of 0.25. Samples were subjected to oedometer compression (in dry state) and taken out at stress levels of 1100, 2200, 8800 & 17600 kN/m² for sieve analysis (to compute B_p, B_T, B_r) and image analysis studies related to changes in particle angularity (see section 4.3). Four sands investigated were standard sand, Ganga sand, kalpi sand & calcareous sand (Table 3 in section 4.3). On the basis of relative breakage index, B_r, it was found that at a stress level of 1100 kN/m², except for calcareous sand (made up of carbonaceous shells), no grain modification was discerned (B_r = .02 for calcareous sand) for other sands. Major increase in B_r values for Ganga, kalpi & calcaceous sands was observed at a stress level of 2200 kN/m². For the stress increase from 2200 to 8800 kN/m², only a small further increase in B_r was observed for Ganga, kalpi & calcareous samples. However, at stress levels greater than 8800 kN/m² (upto 17600 kN/m²) Ganga, kalpi & calcareous sand samples indicated marked increase in B_r values. Stress level of 8800 kN/m² was estimated to be the value at which significant grain crushing commences for these sands. The standard sand, consisting of rounded quartz grains showed B_r = 0 right upto 17600 kN/m². Samples after compression at various stress levels were also examined with the image analyzer to evaluate the changes in grain angularity arising from particle breakage. A typical result for Ganga sand is shown in Fig.34. The distribution of tangents (count of surface protrusions) obtained from image analyzer studies clearly brings out the changes in grain angularity. As pointed out in section 4.3, 4 tangent count was taken to represent rounded particles. The proportion of rounded particles increased from 12 % in unstressed state to 17 % at a stress level of 2200 kN/m² where sieve analysis showed maximum value of B_r. This increase is a clear indication of sharp protrusions being knocked off. It will also be seen that few grains in original sand with tangent count in excess of 28 are totally absent during image analysis after loading to 2200 kN/m². These grains along with other angular ones have contributed to the increased rounded particles. It is also brought out that at a stress level of 17600 kN/m², the grains were split and the proportion of rounded grains has again dropped to around 8 %. Changes in particle shape for Ganga sand were also examined in terms of flatness and elongation

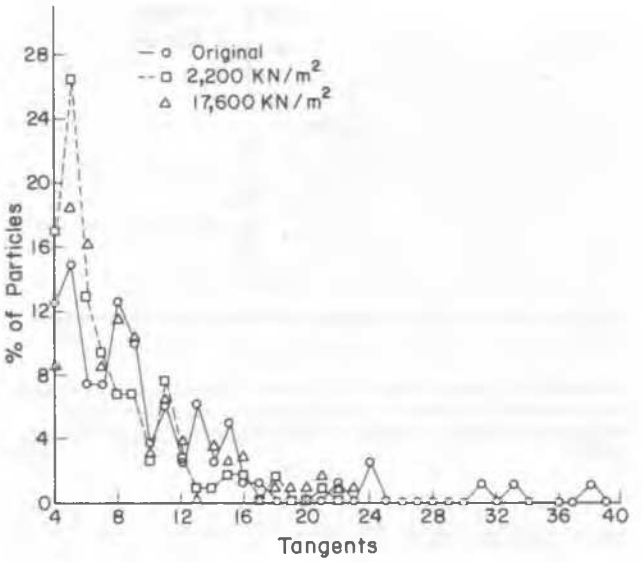

Figure 34. Changes in grain angularity (related to number of tangents) during compression of Ganga sand (from Rahim, 1989).

ratios in Zingg diagram before & after loading upto 2200 kN/m². The unstressed Ganga sand had only 24.4 % particles in quadrant II (Fig. 21) and after compression under 2200 kN/m², this proportion increased to 31 % indicating change in grain shape from plate-like, bladed & rod-like to spheroidal (equant). The breaking off of the grain boundary protrusions has resulted in change of particle shape also.

These results suggest that B_r determination, and image analysis studies suggested here can be successfully used to evaluate the degree of grain modification & the stress level at which these modifications commence. Based on the available data (Castro et al 1982, Vaid & Chern, 1985, Yudhbir & Rahim 1987, Rahim 1989), it may be suggested that the threshold stress, at which a sand undergoes grain modification & therefore changes in behaviour under stress, depends upon its initial relative density, angularity, and mineralogy. More detailed studies on subangular and angular sands are required to establish the relationships between threshold stress and initial relative density for different sands.

5.4 A state variable for sands

"Loose sands and gravels are known to have less resistance to shear than the same soils in a dense state" (Winterkorn and Fang, 1975). A first estimate of the peak angle of friction of a sand might be obtained from charts such as those produced by Winterkorn and Fang (1975), which require knowledge only of the packing of the sand and some basic information about particle shape and size. The packing of the sand is indicated by its relative density I_D:

$$I_D = (v_{max} - v)/(v_{max} - v_{min}) \qquad (32)$$

where v_{max} and v_{min} are so-called maximum and minimum values of specific volume, determined by standard procedures (see, for example, Kolbuszewski, 1948).

However, relative density on its own is not sufficient, since a dense sample tested at a high stress level shows a much lower strength, close to that of a loose sample. Most test data for soils have come from conventional triaxial compression tests in which the cell pressure is held constant with the consequence that, in a drained test, the mean stress level increases from the start of the test until failure occurs. If it is only the strength of sands in conventional triaxial compression tests that is of concern, then it may be acceptable to seek correlation of strength with initial densities and confining stresses. The character of this response has been examined for many sands by Bolton (1986) and he has produced the expression

$$\phi' - \phi_c' = 3\, I_D(10 - \ell n\, p_f') - 3 \qquad (33)$$

as a best fit to a wide range of data, where ϕ_c' is the critical state angle of friction. In this expression, mean stress has to be measured in kPa, and ϕ' in degrees. Bolton suggests that it should only be used where it leads to values of ϕ' in the range $12^o > \phi' - \phi_c' > 0$.

The problem with the use of relative density as an index of sand behaviour is that it is conventionally computed using the specific volume of the sample as it has been prepared, with no confining pressure. Consequently, it does not reflect the changes in volume that may occur either as an initial stress state is applied, or as the sand is sheared.

If a critical state line for a sand

$$v = \Gamma - \lambda\, \ell np' \qquad (34)$$

can be located in the p':v compression plane, then the composite volumetric variable

$$v_\lambda - \Gamma = v + \lambda\, \ell np' - \Gamma \qquad (35)$$

can be calculated at any stage of a test.

An extensive study of the use of the quantity $v_\lambda - \Gamma$ to characterise the strength (and dilatancy) of sands has been made by Been and Jefferies (1985, 1986). They have managed to locate straight critical state lines (they actually call them steady state lines but the two are probably equivalent, see Negussey et al (1988) in the v:ℓn p' compression plane for many different sands and sandy silts, and have calculated values of $(v_{\lambda i} - \Gamma)$, which they call the state parameter, from the volume and mean stress obtaining when the sand is about to be sheared in a triaxial test. Thus they include the effect of the volume change that has occurred as the sample is compressed, but not the effect of dilatancy during shear. The sand strength data that they have accumulated reveal a fairly narrow spread (Fig. 35). As a result, if the initial value of the state parameter $(v_{\lambda i} - \Gamma)$ is known then the peak strength to be expected in triaxial compression tests can be estimated to $\pm 2.5^o$. Subsequent work (Been et al (1986); Been et al (1987) has indicated that

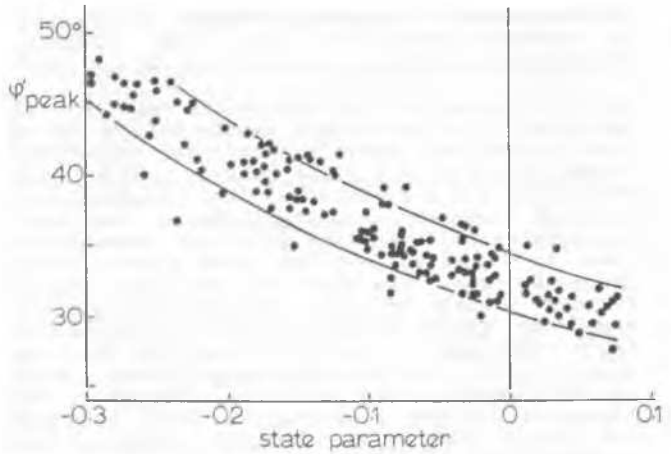

Figure 35. Variation of peak angles of shearing resistance of sands with state parameter (after Been and Jefferies, 1986).

this state parameter ($v_{\lambda i} - \Gamma$) is useful also in understanding results of cone prenetration tests in sands and sandy silts.

However, the use of initial vlaues of ($v_\lambda - \Gamma$) is not satisfactory if a rational picture of sand response is to be built up, because in general volume changes and stress changes on relevant field stress paths (which may bear little resemblance to triaxial compression stress paths) will lead to continuous and major variation in v_λ.

Consideration of data for typical sands shows that the critical state lines that have been estimated can only be considered locally straight in the v: ℓn p' compression plane. If the specific volume v_c on the critical state line, of whatever actual shape, at the current mean effective stress can be determiend, then the quantity $v-v_c$ becomes a more general state variable which has wider application than $v_\lambda - \Gamma$. If the critical state line is straight in the v:ℓn p' compression plane then

$$v_c = \Gamma - \lambda \ell n p' \qquad (36)$$

and

$$v - v_c = v_\lambda - \Gamma \qquad (37)$$

Lee and Seed (1967) report results of conventional triaxial compression tests performed at constant cell pressures between 98 kPa and 12 Mpa. They report triaxial tests on samples prepared at two initial densities, and isotropic compression tests on samples prepared at four initial densities.

From the available compression plane information an approximate location for a curved critical state line in the compression plane can be suggested and this has been used to calculate values of v_c for particular values of mean effective stress. The failure data reported by Lee and Seed are presented in Fig. 36 in terms of peak angle of friction as a function of $v_f - v_c$, calculated from the failure values of specific volume. An approximate description of

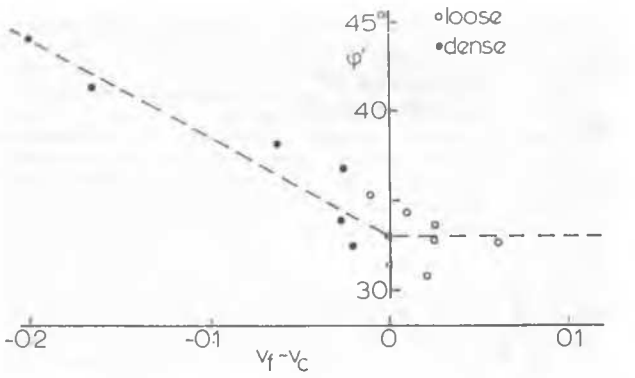

Figure 36. Dependence of peak angle of shearing resistance on state variable at failure for Sacramento River sand (data from Lee and Seed, 1967).

these failure data would be

$$\phi' - \phi_c' = -55(v_f - v_c) \text{ for } v_c > v_f \qquad (38)$$

$$\phi' - \phi_c' = 0 \text{ for } v_c < v_f \qquad (39)$$

where ϕ' is measured in degrees. The second expression is essentially redundant because samples with $v > v_c$ are not expected to show a peak before the critical state is reached. The expectation from the work of Been and Jefferies (1985, 1986) is that these relationship would hold for samples of this sand prepared at any initial density.

Compelte test paths for two tests on initially dense and two tests on initially loose samples are shown in a $(v - v_c)$:q/p' plot in Fig. 37. The loose sample tested at low pressure, and the dense sample tested at a moderately high pressure show essentially no change in state variable $(v - v_c)$ as they are sheared : they start and remain very close to the critical state line in the v:ℓn p' plane. The dense sample tested at low pressure rises to a peak and then heads down towards the critical state. The loose sample tested at high pressure rises steadily towards the critical state.

Plotting information in terms of q/p' and $(v - v_c)$, whether v_c is deduced from a straight or a curved cirtical state line, brings togehter data from samples with widely differing densities. The state variable $(v - v_c)$ introduces mean effective stress in a rational way and in particular allows some note to be taken of the current values of mean stress and volume which may be very different from their initial values.

Relative density is not a sufficient quantity for characterising sand behaviour. It might be suggested that $(v - v_c)$ should be normalised by dividing it by $(v_{max} - v_{min})$ in order to produce a composite state variable which can bring together data for sands of widely differing mineralogy, angularity, and particle size (compare Hird and Hassona, 1986; Been and Jefferies, 1986). The specific volume range $(v_{max} - v_{min})$ gives an indication of the range

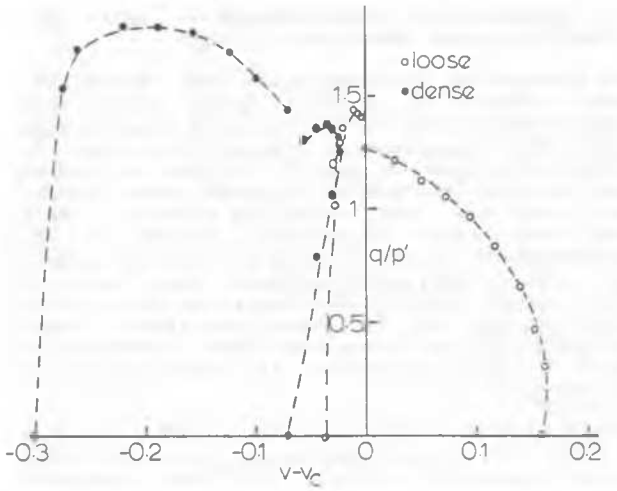

Figure 37. Triaxial test paths for Sacramento River sand (data from Lee and Seed, 1967).

of packings available at low stress levels, but does not appear to relate directly either to the slope of the critical state line at low stress levels, or to the slope of isotropic compression curves at higher stress levels, where particle modification becomes important - and these are both factors that, through the state variable ($v - v_c$), appear to have a controlling infleunce on sand behaviour in general and on the strength of sands in particular.

These concerns are best illustrated through a close examination of the data on Steady State Line, SSL, for variety of sands (Fig. 38) reported by Castro et al (1982). Similar results are reported by Vaid and Chern (1985) for tailings sand and Ottawa sand.

These results establish general patterns of the shape of SSL for angular to subangular and rounded to subrounded sands. While the subrounded to rounded quartz sands do not show any change in slope of SSL upto 1000 kN/m², irrespective of the value of initial relative density, the SSL for subangular to angular sands undergoes change in slope even at stress level of 100 kN/m² depending on the value of initial relative density of the sample. The slope of SSL for subrounded to rounded sands varies from 0.03 to 0.06 for the effective stress at steady state varying from 10-1000 kN/m². For subangular to angular sand the slope of SSL is 0.06-0.08 for stress level of 10-100 kN/m², 0.08-0.17 for 100-200 kN/m², 0.19 for 200-400 kN/m², and about 0.35 for stresses greater than 400 kN/m². Incidently for a steady state stress level of 400 kN/m², for tailings sand at an initial relative density of 0.3, the value of consolidation stress (for the same value of v) is 2000 kN/m². As shown in section 5.3, at these stress levels, subangular to angular sands experience maximum grain modification, which has significant effect on their compressibility & shear strength.

It is important to note that at these stress

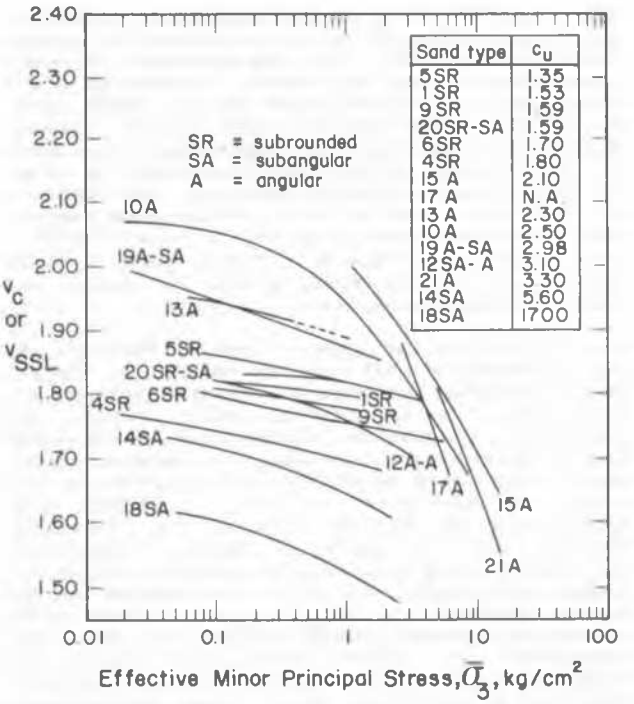

Figure 38. Family of steady state lines for sands with different angularity and gradation (from Castro et al, 1982).

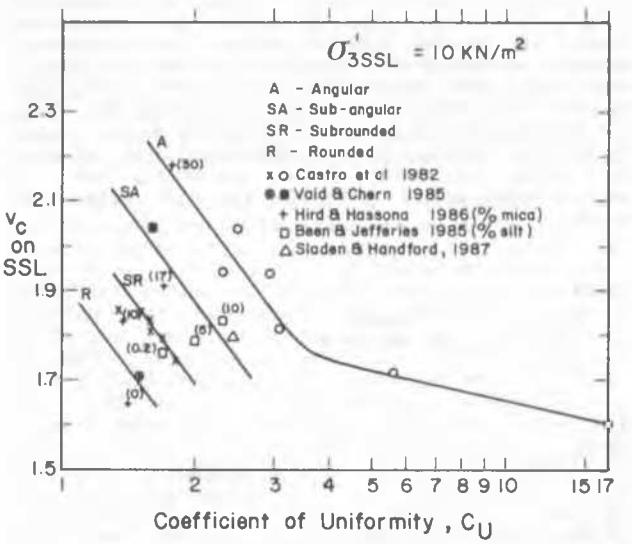

Figure 39. Relationship between specific volume at steady state, angularity and gradation.

levels only breakage of sharp edges or protrusions on grain boundary occurs without any crushing of sand particles; the rounded grain show absolutely no changes in grain geometry or size (Vaid & Chern, 1985; Rahim, 1989). Therefore the position and slope of the SSL of a sand tested at consolidation pressure

less than 2000 kN/m² is expected to be significantly controlled by the grain angularity and gradation (Fig., 39). For the purposes of discussion here, $\sigma_{3\ SSL}$ is chosen (instead of p') since the data from Castro et al (1982) and Vaid & Chern (1985) is in terms of this stress parameter. For other data shown in Fig. 39, the value of p' at SSL, corresponding to the reference $\sigma'_{3\ SSL}$= 10 kN/m² (adopted) was computed from the value of angle of shearing resistance at steady state reported for these sands. For Castro's & Vaid & Chern's data trends similar to the one shown in Fig. 39 exist at higher stress levels also.

In the light of the trends shown in Fig. 39, it may be observed that, in the range of stress levels commonly employed in triaxial testing of sands in the laboratory, only sands of comparable angularity, gradation & mineralogy may be expected to give SSL in a narrow range where they could be normalized in terms of a state variable such as $v-v_c$. There are indications that for the same initial relative density, $(v-v_c)/(v_{max}-v_{min})$ may be comparable for sands having similar grain angularity, mineralogy, and gradation. In case of subangular to angular sands $(v-v_c)/(v_{max}-v_{min})$ increases with increasing stress level whereas in case of subrounded to rounded sands this ratio is independent of stress level upto 2000 kN/m². More data is needed to verify these indications.

For 40 shows the variation of specific volume range $(v_{max}-v_{min})$ with angularity and gradation of sands. Solid lines are based on data from Youd (1973) tested against results for variety of sands. On the basis of results shown in Figs. 39 & 40, it may therefore be suggested that, at stress levels below the treshold stress (where grain modification is maximum), angulrity and gradation of sands uniquely govern the range of packing available at very low stress levels and also the position & slope of the SSL (CSL). These considerations should be borne in mind while searching for a generalized state variable for all types of sands.

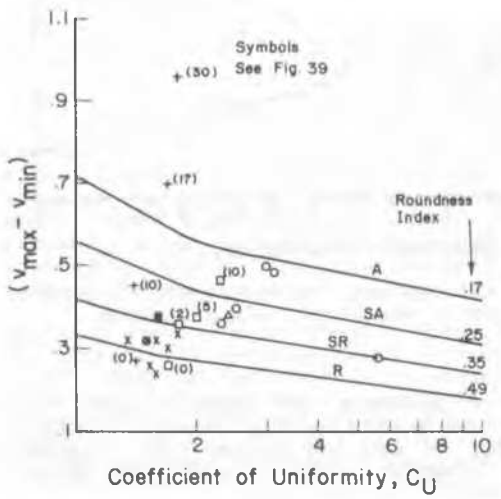

Figure 40. Relationship between specific volume range, angularity, and gradation for sands.

5.5 Generalized relationships & Very low effective stress behaviour of clays

The concepts of Critical State Soil Mechanics, CSSM, provide a rational frame work that enables the formulation of a valid constitutive model for resedimented soils in states of effective stress and specific volume, v, higher than critical states. It has been shown (Skempton & Northey, 1952; Schofield & Wroth, 1968) that void ratio or specific volume can be generalized by converting to a liquidity index, I_L , basis. Many attempts have been made to evolve generalized relationships in terms of I_L, effective stress, p', and undrained shear strength c_u, for remoulded clays (Skempton & Northey, 1952; Leroueil et al, 1983; Carrier et al, 1984).

Schofield (1980) suggested the simple division of behaviour at limiting states into three different classes of failure - fracture, rupture, and yield. Schofield further argued that at specific volume corresponding to plastic limit, the effective stress p'at critical state is ten or more times (he adopted a factor of ten) more than the effective pressure or suction in the plastic limit thread when it is made to crumble in the index test. This assumption based on available triaxial test data, examined in terms of intersection between Coulomb and no-tension (q/p'= 3 compression, -1.5 in extension) criterion, helped to establish the width of the band in which one can expect to observe Coulomb rupture behaviour. An equivalent liquidity index was proposed to express the combination of specific volume and effective stress which determines whether a soil in the ground will fracture, rupture, or yield.

The fracture-rupture boundary suggested by Schofield (1980) in a sense ascribes effective pressure or suction values to the liquid limit, W_L, and plastic limit, W_p, as determiend in index tests. Croney & Coleman (1954) have measured suction values on actual samples used in the determination of liquid & plastic limits. Water content-suction relationships for soils and sand-mineral admixtures in continuously disturbed or remoulded states have been reported by Croney & Coleman (1954), and Dumbleton & West (1970). Results of suction measurements on soils in initially slurried and undisturbed states are also available (Croney & Coleman, 1954). In the following discussion generalized relationships for remoulded clays have been examined on the basis of simple suction measurements & index tests. The mode of failure at very low effective stresses obtaining in remoulded samples has been reviewed in the light of fracture-rupture boundary suggested by Schofield (1980).

Suction measurments (Figs. 41, & 42, 43) in initially slurried state (Curve D), continuously remoulded state (curve G), and undisturbed state (Curve A) may be transformed into I_L: log p' plot as depicted in Figs.44 & 45. The data for initially slurried state may be interpreted as the generalized Virgin Consolidation Line, VCL, for resedimented clays. In fixing the position of VCL, the commonly accepted ratio of 100 between values of p' at I_L = 0 & I_L = 1 has been assumed, and p' at I_L = 1.0 has been taken as 6 kN/m² (6-10kN/m² in Fig. 44). Based on the

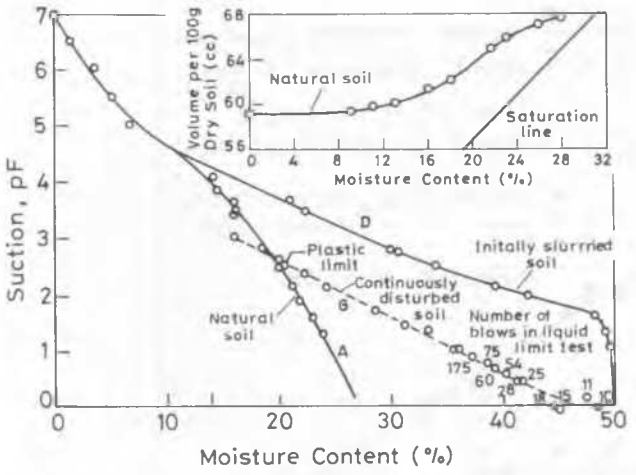

Figure 41. Suction-moisture content relationship for light clay (from Croney and Coleman, 1954).

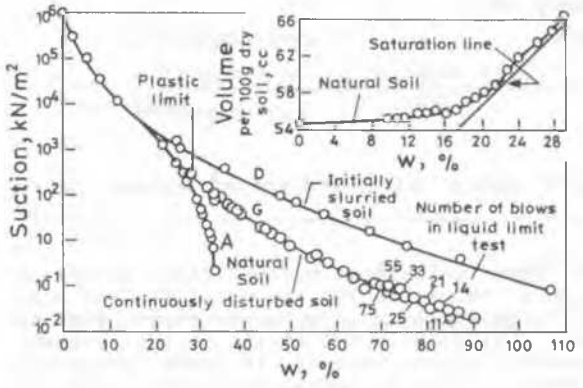

Figure 42. Suction-moisture content relationship for heavy clay (from Croney and Coleman, 1954).

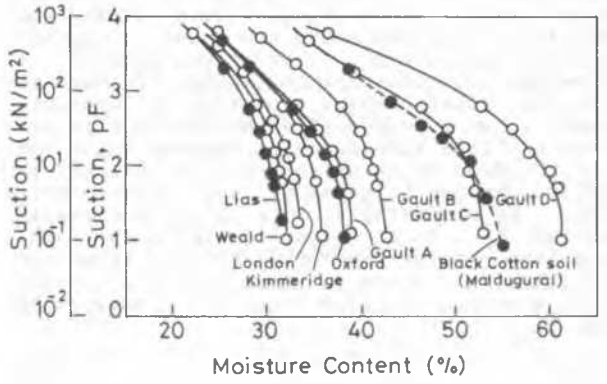

Figure 43. Suction-moisture content relationship for undisturbed clays (from Croney, 1977).

interpretation of consolidation data (Skempton, 1953), the value of vertical effective stress, σ_v' on K_o -line can be converted into the corresponding p' on VCL through the use of K_o = (1-Sin ϕ') and Modified Cam Clay model. The values of p' at I_L = 1.0 range between 6-15 kN/m². The values of σ_v'= 6.3 kN/m² (Wroth & Wood, 1978) 7 & 8 kN/m² at I_L= 1.0 (Biarez, et al, 1989) on K_o - line would also give p' values in the range of 6-15 kN/m². For the purpose of investigating a correlation between slope of VCL & soil plasticity index, I_p, p' = 6 kN/m² at I_L = 1.0 will be assumed in this presentation.

The generally accepted linearity of VCL between I_L = 1 to 0, tacitly assumes that soils were actually resedimented from an initially slurried state (initial water content, W_o, greater than liquid limit). Available data from isotropic consolidation tests on resedimented soils suggests significant dependence of critical state parameter, λ (related to slope of generalized VCL), on the initial moulding water content, W_o. λ increases as W_o increases upto 2.5 times W_L; the effect being more pronounced for soils with high plasticity index. This effect was recognised by Bjerrum (1954) when he emphasized that Hvorslev effective cohesion (c_e') coefficient, c_e'/p_e' is constant for a clay only if the equivalent consolidation pressure, p_e', is estimated from a consolidation curve obtained from a test on initially slurried sample with $W_o > W_L$. The assumed linearity also neglects the effect of stress level. Review of the shape of consolidation curves for a variety of soils published in the literature indicates that in the vicinity of I_L = 0, the consolidation curve starts becoming concave upwards and the deviation from linearity increases with increasing stress level beyond p' corresponding to I_L = 0. It is also observed that for p' less than that at I_L = 1, the slope of the consolidation curve for slurried samples ($W_o > W_L$) is steeper than the linear extension of VCL. However, inspite of these limitations the effective stress range over which VCL is linear is quite significant since the value of p' at I_L = 0 would represent an in-situ effective overburden pressure of 800 kN/m².

Fig. 44 also shows the I_L: p' relationship for continuously remoulded samples of clays & sand: mineral admixtures. In order to correctly interpret I_L : p' and I_L : c_u relationships for remoulded soils, it is important to distinguish between the structure of clays in totally remoulded state as compared to that obtained in resedimented samples. Coleman & Croney (1954) have argued that the effective stress (or suction) values corresponding to W_L or W_p during index tests cannot be evaluated from the suction-water content relationships (or isotropic consolidation curve) obtained from the initially slurried samples since, "the soil is in an entirely different structural condition" during this test compared to that during index tests (see also Seed et al, 1964, Schofield, 1980). Leroueil et al (1985) have also emphasized the need to distuinguish between destructured, remoulded & resedimented states of clays with reference to attempts to formulate generalized relationships in terms of I_L & c_u for remoulded soils. It is therefore important to note that the values of p' at water content equal to liquid limit & plastic limit, as obtained from VCL, are significantly different from those obtained from suction measuremetns made by Coleman & Croney (1954) & Dumbleton & West (1970) at various stages of actual index tests.

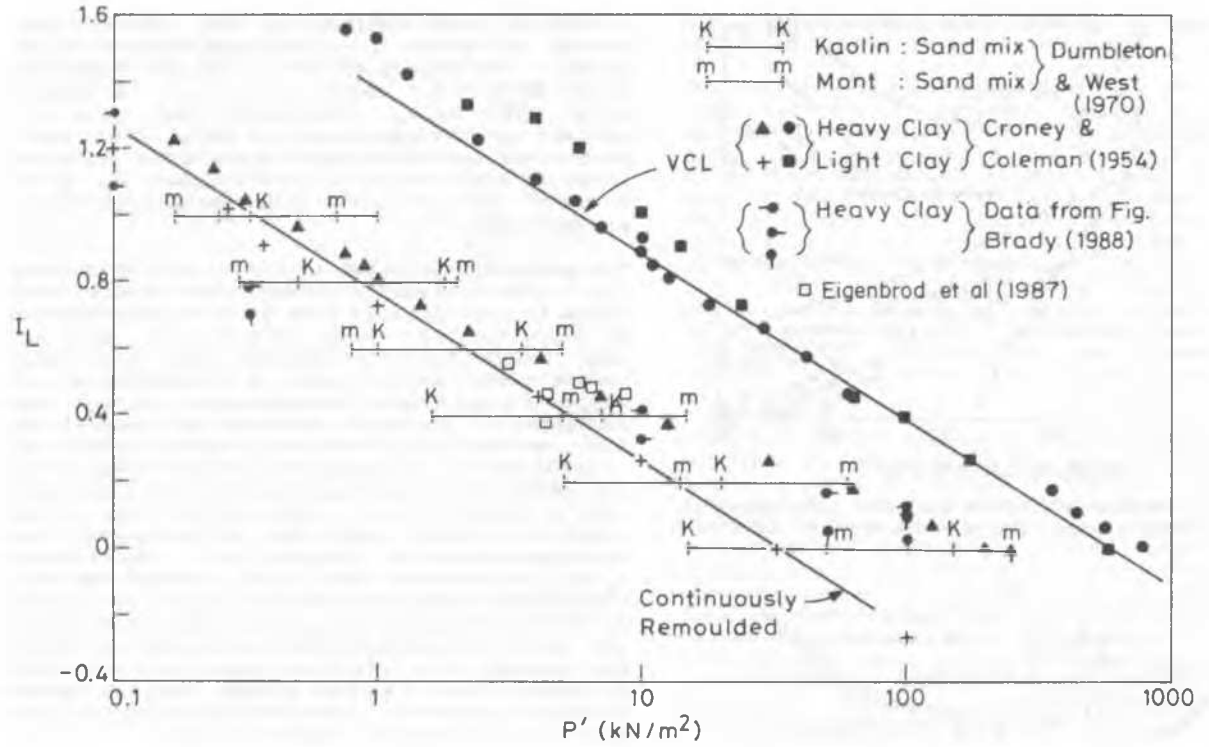

Figure 44. Normalized relationships between liquidity index and p' for resedimented and continuously remoulded clays.

The I_L : p' relationship for continuously remoulded state may be represented by a line parallel to VCL and is interpretted as the fracture-rupture boundary as suggested by Schofield (1980). As will be shown later in this section the value of p' in the continuously remoudled state is order of magnitude smaller than the corresponding value at Critical State Line, CSL. Data from Fig. 43 has been replotted in I_L : log p' space in Fig. 45. Some observations are important.

(i) I_L : log p' relationship represents reloading from a fully unloaded state and the trends exhibited are typical of the behaviour observed during reloading from very low stress levels. Under these conditions the hysteresis loop between unloading & reloading curves is expected to be maximum.

(ii) Data points show no consistent trend with I_p (varying from 0.36 to 0.89).

(iii) At I_L = 0, the values of p' lie in a very narrow range. In fact the scatter would be further reduced if all samples had in-situ water content at their respective plastic limit value. It may be noted that majority of the undisturbed soils (except Black Cotton, likely to be dessicated) are stiff overconsolidated British clays and are likely to be at in-situ water content close to their respective plastic limit. Data for remoulded Bearpaw shale, London clay, and Bangkok clay isotropically unloaded from p' at I_L = 0 on the VCL, lies in a narrow range in the unloading zone shown in Fig. 45.

Given that unloaidng curves from different maximum p' values on VCL are parallel, and p'at I_L = 0 on VCL lies in a narrow range and an average value (p' = 600 kN/m² in the present discussion) can be assumed, it seems reasonable to expect that a normalized I_L : log p' unloading - reloaidng relationship, starting from I_L = 0 on VCL, also exists for a variety of resedimented clays (Fig. 45).

Generalised relationships for clays in resedimented state (VCL & Unload-reload line) and completely remoulded state are shown in Fig.46. Reference pressure p' = 1 kN/m² was adopted to derive the relationships indicated. In case of unloading relationship, the value of specific volume, v at p' = 1.0 kN/m² on the appropriate unloading line (depending on maximum value of p' on VCL from which unloading is done) can be readily derived in terms of the relationship shown. By comparing v : ℓn p' relationship with the I_L : ℓn p' equations (Fig. 45) and using the definitions of I_L & v in terms of void ratio, e, it can be shown that the slopes of VCL & unload-reloaded lines are respectively given as

$$\lambda = 0.217\ G_s\ I_p \qquad (40)$$

$$\kappa = 0.048\ G_s\ I_p \qquad (41)$$

Using the G_s, I_p values for 34 soils listed by Croney (1977), an average value of G_s = 2.72 in equations (40) & (41) yields

$$\lambda = 0.59\ I_p \qquad (42)$$

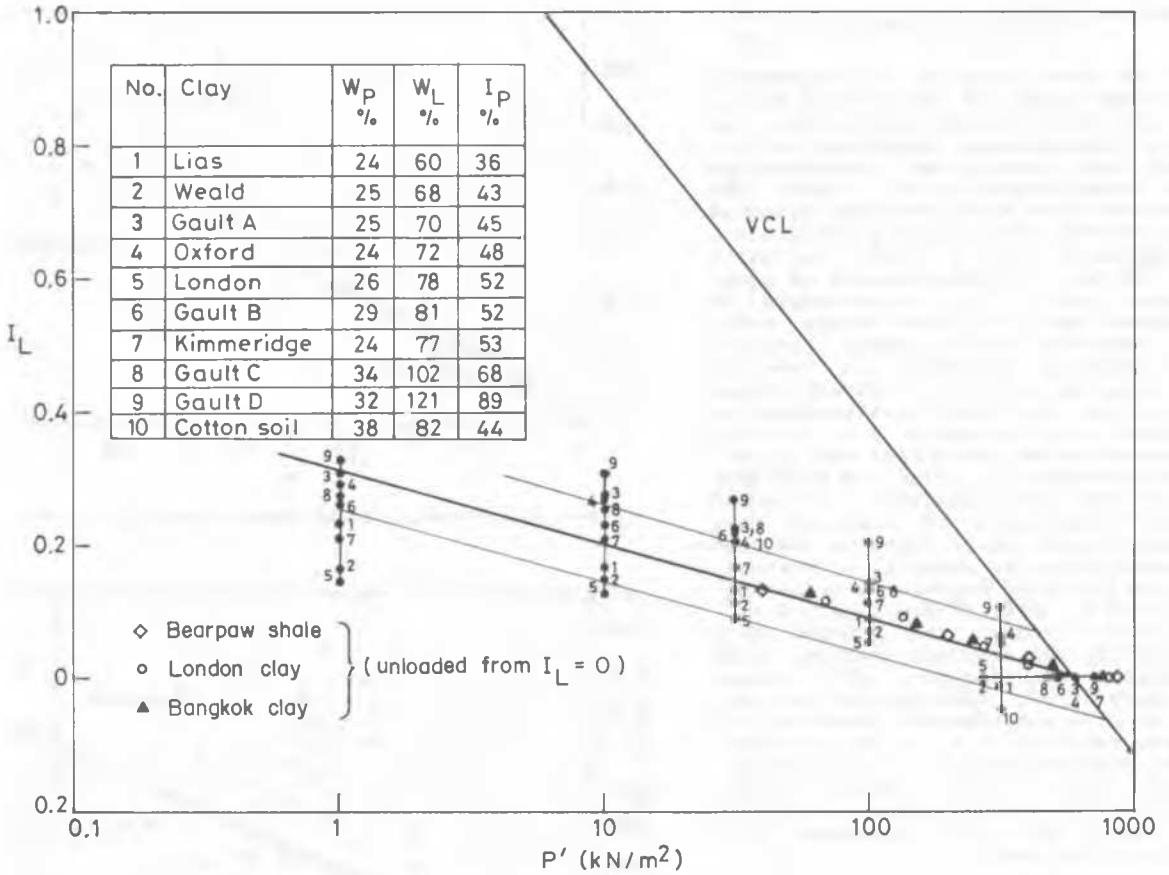

Figure 45. Normalized unloading-reloading line for resedimented clays.

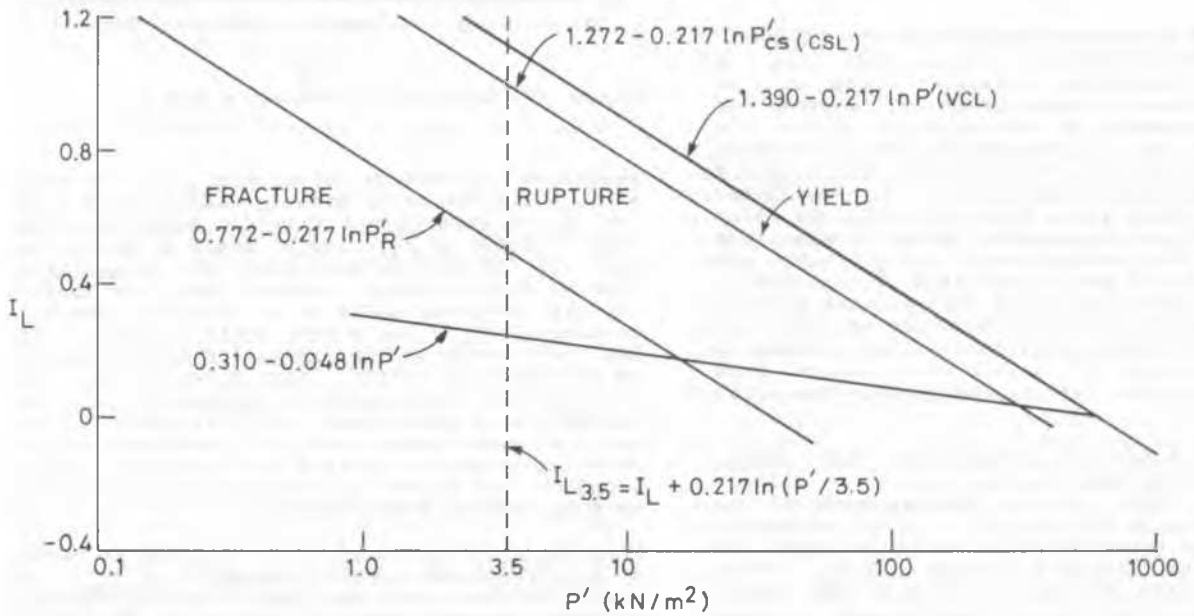

Figure 46. Normalized VCL, CSL, fracture-rupture boundary, and unloading-reloading lines for clays.

$$\kappa = 0.131\ I_p \qquad (43)$$

Figs. 47 & 48 show results of regression analysis for large number of soils (from Mayne, 1980, 1981, and other sources) along with the $\lambda : I_p$, $\kappa : I_p$ relationships (equations (42) & (43)) derived from generalized relationships proposed for resedimented soils. Given the variety of sources from which data was obtained, the agreement between statistical predictions & that from equations (42) & (43) is quite encouraging. While $\lambda : I_p$ relationship is generally accepted, the $\kappa : I_p$ relationship is usually observed implicitly even though every geotechnical engineer would expect greater recovery on isotropic unloading in case of resedimented soil of high I_p. A direct consequence of $\lambda : I_p$ & $\kappa : I_p$ linear relationships is that the critical state parameter $\Lambda = (1-\kappa/\lambda)$ cannot be expected to be correlated with I_p or critical state parameter M. Figs. 49 & 50 show the results of regression analysis. It would therefore seem reasonable to conclude that Λ or Λ_o - (back calculated by Mayne on the basis of shear strength data for normally & overconsolidated clays) do not show any correlation either with I_p or M. Fig. 51 combines Λ & Λ_o values and it is evident that both these values obtained by two separate methods show similar unrelated variation with M. Λ values for 75 soils show normal distribution with a mean value of 0.76 and standard deviation of 0.12. The mean value of Λ = 0.76 is quite close to 0.78 obtained from $\Lambda = 1-\kappa/\lambda$ using the equations (42) & (43). Wroth (1984) purposes Λ = 0.8 for a wide variety of clays. Furthermore, Mayne (1980, 1981) suggests that a relationship of the form

$$\frac{(c_u/\sigma'_{vo})\ \text{overconsolidated}}{(c_u/\sigma'_{vo})\ \text{normally consolidated}} = (OCR)^{\Lambda} \qquad (44)$$

can be used to estimate variation of (c_u/σ'_{vo}) with overconsolidation ratio, OCR (σ'_{vo} is effective overburden stress). Ladd et al (1977), who used a superscript 'm' instead of Λ_o or Λ, suggested an average value of m = 0.8 (0.75 -.8) to fit results for soils with I_p varying from .21 to .75 (Fig. 52a) (for soils X & Y see Parry & Wood, 1982). The predicted values for these soils with Λ = 0.78 (Fig. 52b) seem to give a reasonable order-of-magnitude estimate of the variation of (c_u/σ'_{vo}) with OCR for a variety of soils (see also Wroth, 1984). These considerations would suggest that for the purposes of an order-of-magnitude estimate of resedimented soil behaviour, the suggested average value of Λ = 0.78 & λ, κ values from equations (42) & (43) may be used in Cam Clay models.

With Λ = 0.78 and the Modified Cam Clay model, it can be shown that $p'_e/p'_{cs} = (2)^{\Lambda} = 1.72$ or $p'_{cs}/p'_e = 0.58$. p'_{cs} is the value of p' on CSL. The value of $p'_{cs}/p'_e = 0.58$ generally lies in the experimentally evaluated range of 0.5-0.6 (see Schofield & Wroth, 1968). Wroth (1984) proposes $p'_{cs}/p'_e = 0.5$ for a wide variety of clays. With p'_e = p' on VCL, and at I_L = 1.0 p'_e = 6 kN/m², the corresponding value of p'_{cs} works out to be 3.5 kN/m². Parry & Wood (1982)

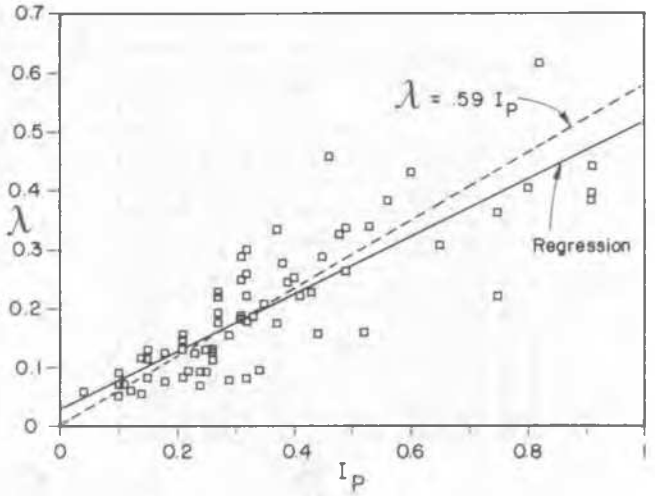

Figure 47. Correlation between λ and I_p.

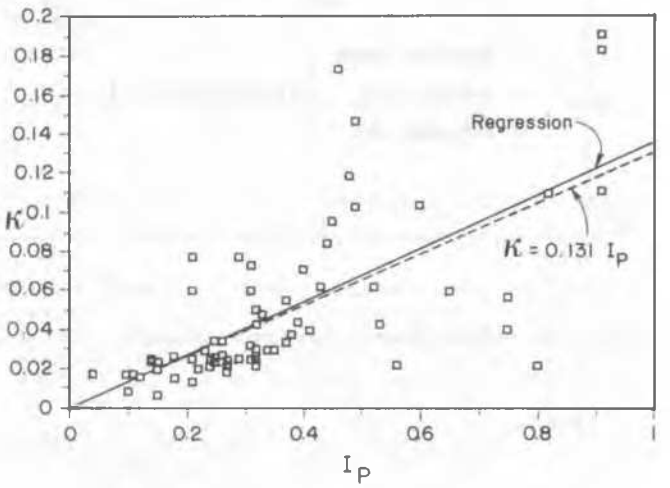

Figure 48. Correlation between κ and I_p.

suggested an average value of p'_{cs} = 3.3 kN/m² at I_L = 1.0 for soils with I_p ranging from 0.15 to 1.0. A generalized Critical State Line is thus located in I_L : log p' space as shown in Fig. 46. It will be seen that the interpretation of suction-water content data for continuously remoulded soils as a fracture-rupture boundary on I_L : log p'map, would predict one log cycle width of the rupture zone as suggested by Schofield (1980). Also shown in Fig. 46 is the line recommended by Schofield for the estimation of equivalent liquidity index. The suction measurement data on remoulded soils thus independently locates the fracture-rupture boundary and cannot be expected to lie on CSL as suggested by Brady (1988).

With $p'_{cs}/p'_e = 0.58$, $p'_{fr}/p'_e = .058$ (p'_{fr} is value of p'on fracture-rupture boundary), $q_{cs}/p'_{cs} = M$ (q_{cs} is q on CSL), and the fracture-rupture boundary (in q-p' space) fixed by the intersection of Coulomb & no-tension cut off (q_{fr}/p'_{fr} = 3 in compression) criterion, the values of q/p'_e

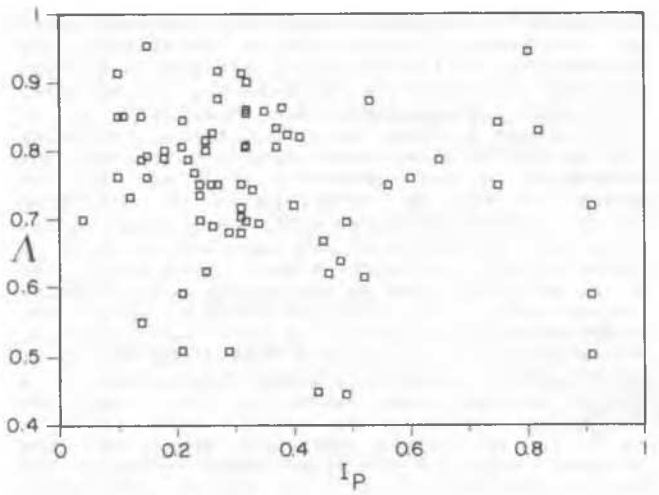

Figure 49. Scatter diagram in terms of Λ and I_p.

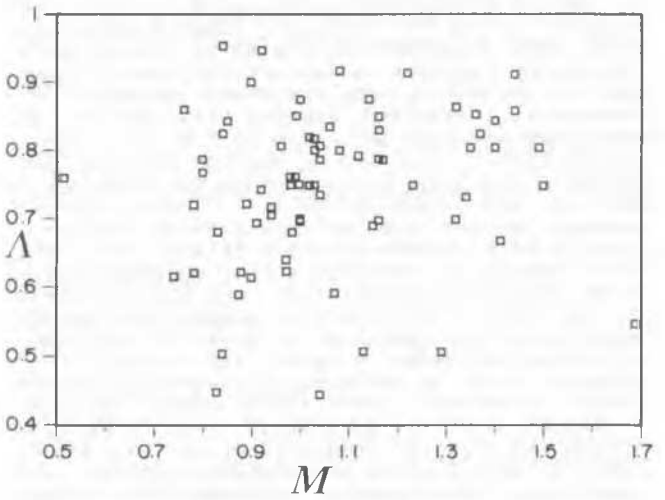

Figure 50. Scatter diagram in terms of Λ and M.

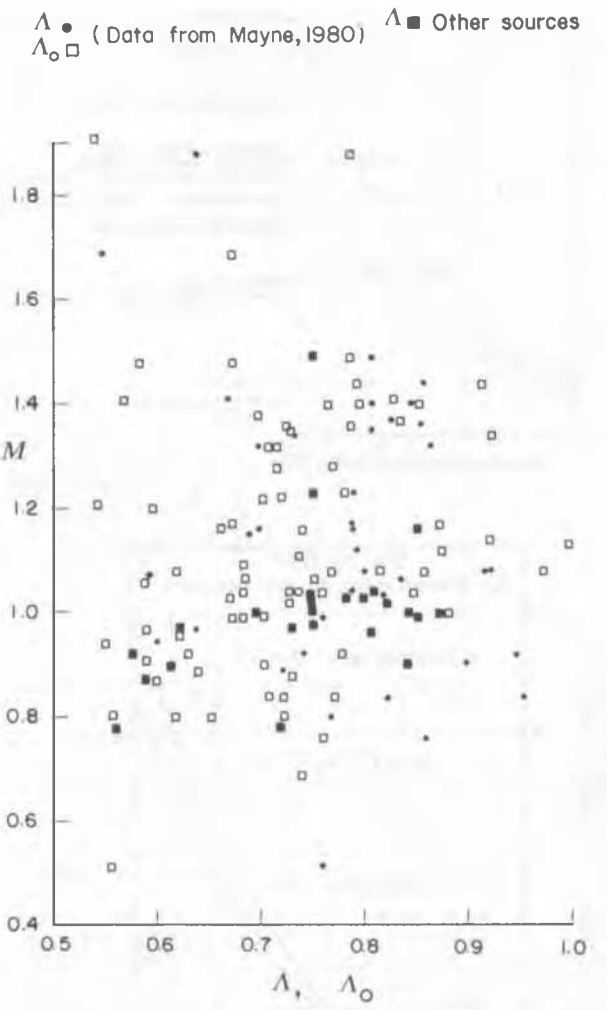

Figure 51. Scatter diagram in terms of Λ, Λ_o and M.

corresponding to critical state & no-tension cut off state in q/p'_e vs p'/p'_e plot can be obtained as:

$$q_{cs}/p'_e = M\ (p'_{cs}/p'_e) = 0.58\ M \qquad (45)$$

$$q_{fr}/p'_e = 0.058 \times 3 = 0.174 \qquad (46)$$

Using I_p: Sin ø' relationship (Mitchell, 1976) the value of q_{cs} at $I_L = 1.0$ works out to be 2.68 kN/m² for a soil with Ip = 1 and 5 kN/m² for a soil with $I_p = 0.1$. The value of undrained shear strength, c_u for resedimented soil on CSL at $I_L = 1.0$ lies between 1.34 to 2.5 kN/m² which agrees well with an average value of 1.7 kN/m² suggested by Wroth & Wood (1978). The corresponding value of c_u for remoulded soil on no-tension cut off at $I_L = 1.0$ is 0.52 kN/m². The remoulded shear strength at a given value of liquidity index is thus unique & does not depend on soil index properties such as I_p (see Skempton & Northey, 1952; Leroueil, et al, 1983). Using a ratio of 100 between the values of c_u (on CSL & fracture-rupture boundary) at $I_L = 0$ & $I_L = 1$, the generalized I_L : log c_u relationships are indicated in Fig. 53.

Two clearly separate generalized relationships in I_L:log c_u space corresponding to resedimented samples (on CSL) and remoulded samples (on fracture-rupture boundary or no-tension cut off) bring out the importance of making clear distinction between resedimented & remoulded shear strength of soils as emphasized earlier. It may be pertinent to recall that the procedure used to prepare remoulded samples for shear strength determination at different values of I_L (Dumbleton & West, 1970) would produce soils at very low effective stresses (dry state) compared to effective stresses in samples prepared at the

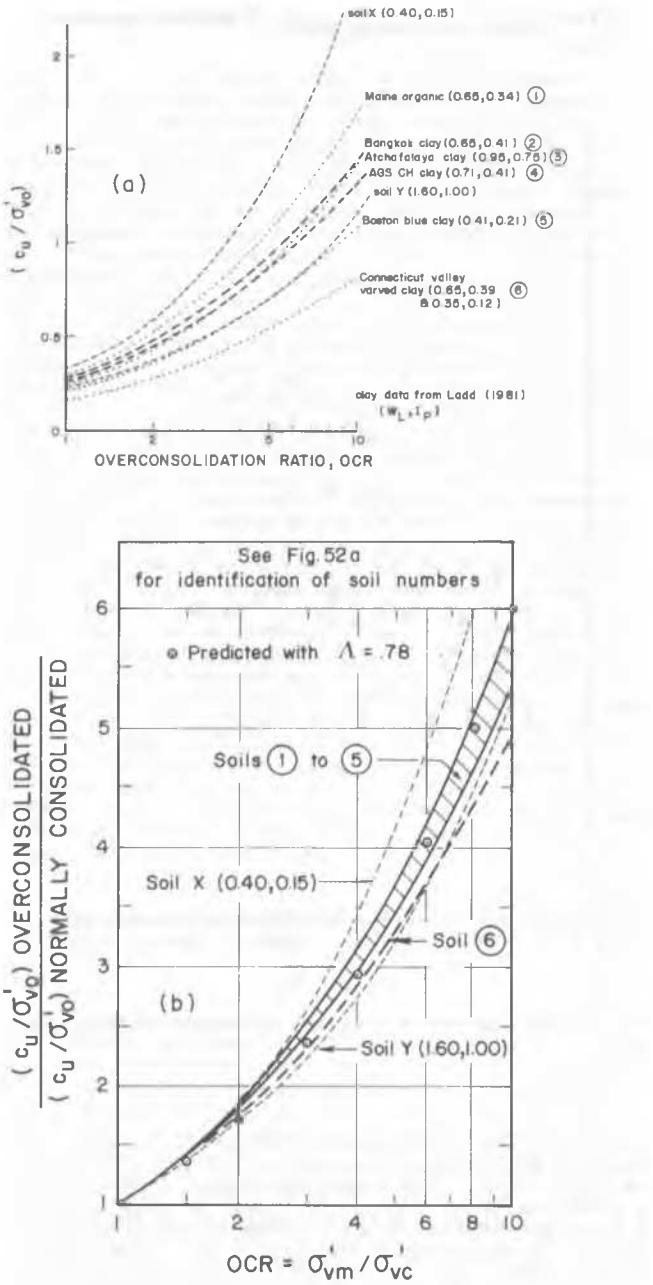

Figure 52. Normalized experimental and predicted relationships between (c_u/σ'_{vo}) and OCR.

same I_L through resedimentation (wet state). While the wet samples would yield on Roscoe surface (see data for resedimented samples in Fig. 53) and those in the rupture band (Fig. 46) would undergo Coulomb rupture on Hvorslev surface (ultimately approaching critical state); the samples in dry state at very low effective stresses would undergo brittle fracture and the failure points would lie on the no-tension cut off in q-p' space & fracture-rupture boundary in the I_L: log p' map rather than on the CSL (see data for remoulded soils in Fig. 53).

The data from special tests (q = constant with p' decreasing) carried out to investigate the possibility of failure being reached in a slope at very low effective stresses due to seasonal variation of pore pressure (Eigenbrod et al 1987), shown in Figs. 46 & 53, clearly validates the interpretations made regarding the very low effective stress behaviour of clays on the basis of suction measurements on remoulded soils. Stiff fissured overconsolidated soils involved in mud flows are expected to be in a continuously remoulded state. Data point for a coastal mud flow on the London Clay Cliffs (Hutchinson, 1970) is also shown in Fig. 53. Shear strength value of 7.4 kN/m^2 was taken for the softer part of the mud flow (from Fig. 6 of Hutchinson's paper) at depth less than 2 m where maximum water content is 0.49, and for the given average values of W_L = 0.85, and W_p = 0.3, I_L is 0.346. It would seem that the minimum value of undrained shear strength of soils involved in mud flows may be reasonably estimated from line x-x shown in Fig. 53 on the basis of the value of liquidity index for the softer parts of the mud flows.

It may be argued that in I_L : log c_u map, the failrue points for tests on samples starting from VCL (resedimented state) or those with equivalent liquidity index greater than 0.6 may lie on the CSL whereas the shear strength of completely remoulded samples will lie on or near the x-x line indicated in Fig. 53. One unique line in I_L : log c_u map for both resedimented & remoulded soils is thus not possible. The so called scatter in I_L : log c_u plots perhaps arises from the fact that no distinction is made between strength values obtained from samples in remoulded state, resedimented state and destructured state (see also Leroueil et al 1985). Much work is needed to better understand the behaviour of clays at very low effective stresses. However, the suction measurement tests as described by Croney & Coleman (1954), Dumbleton & West (1970) appear to offer a simple tool to investigate low effective stress behaviour of remoulded soils. Incorporation of such suction measurement tests in the laboratory investigation program for clays needs to be given a serious consideration.

6. PAPERS SUBMITTED TO THIS SESSION

In presenting the papers submitted to this session, we decided to classify the papers according to various aspects related to laboratory strength and deformation testing as discussed in this report, and to note as to how they match up with various areas of development Accordingly various papers have been classified as follows:

Automation	16, 20, 29
Instrumentation	11
Apparatus	4, 9, 17, 28, 31, 32
Techniques of testing	2, 4, 5, 6, 9, 13, 18, 19, 27
Effects of rotation of principal axes	8, 17, 23, 26, 30, 32

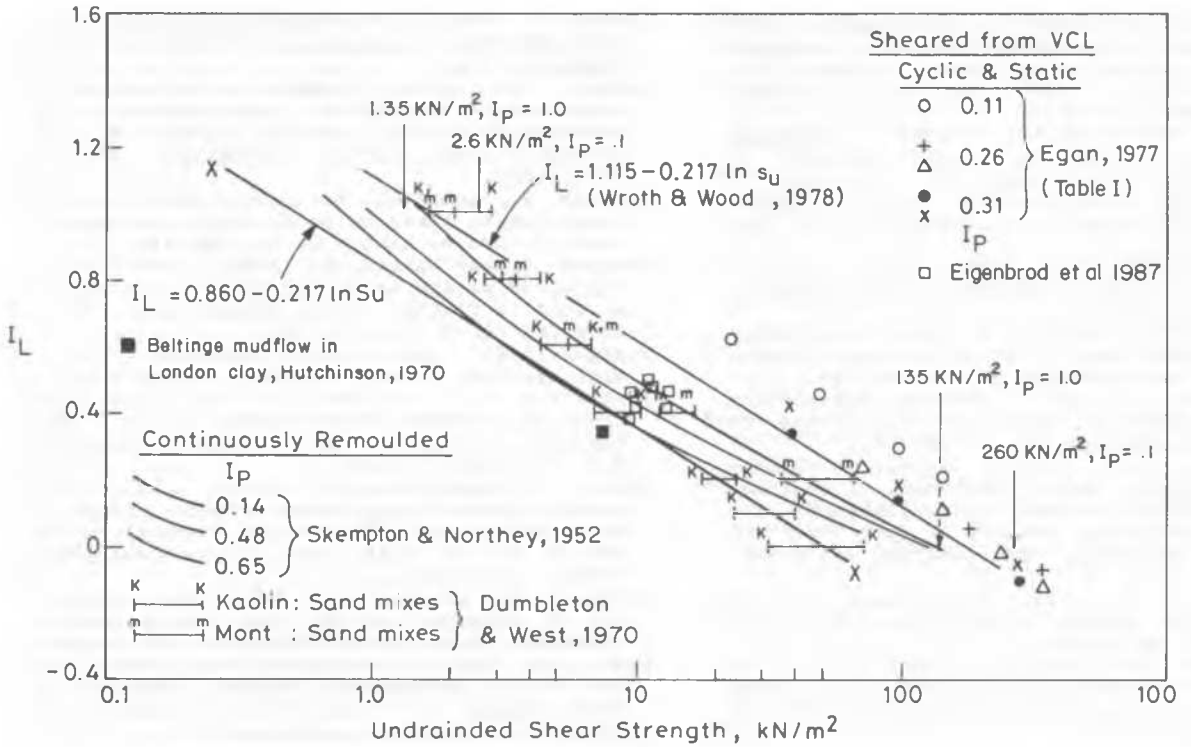

Figure 53. Normalized relationships between liquidity index and undrained shear strength for clays.

Effects of time : 15

Effects of repeated loading : 1, 3, 6, 8, 10, 22, 32

Constitutive relations : 2, 3, 23, 31, 33, 34

Others : 13, 21, 25

The numbers refer to the list of papers as arranged in appendix.

7. CONCLUDING REMARKS

Laboratory testing to determine soil parameters cannot be separated from the models of soil behaviour for which those soil parameters are deemed approproate. As improved instrumentation enables us to make more accurate measurements, and as our technical ingenuity makes it possible for us to test soil samples in new and different ways, so our understanding of the detailed characteristics of the behaviour of soils has improved. The range of applicability of traditional models may have become curtailed, but our increasingly powerful computing resources make it feasible to consider the use of more realistic models in analysis of routine geotechnical problems.

REFERENCES

Adachi, T., et al. (1987). Mathematical structure of an overstress elastoviscoplastic model for clay. Soils and Foundations 27, 3, 31-42.

Airey, D.W., et al. (1985). Some aspects of the behaviour of soils in simple shear. Chap 6 in Developments in soil mechanics and foundation engineering -2: Stress-strain modelling of soils. (eds P.K. Banerjee and R. Butterfield) Elsevier Applied Science Publishers. 185-213.

Alawaji, H., et al. (1987). Experimental observations of anisotropy in some stress controlled tests on dry sand. IUTAM/ICM Symp. on Yielding, damage and failure of anisotropic solids, Grenoble. Cambridge Univ. Engineering Dept., Report CUED/D-SOILS/TR198

Alawi, M.M. (1988). Experimental and analytical modelling of sand behaviour under nonconventional loading. PhD thesis, University of Colorado, Boulder.

Al-Tabbaa, A. and Wood, D.M. (1989). An experimentally based "bubble" model for clay. Numerical models in Geomechanics NUMOG III (eds S.Pietruszczak and G.N. Pande) Elsevier Applied Science 91-99.

Ansal, A.M. and Tuncan, M. (1989). Consolidation in clays due to cyclic stresses. Proc. 12th ICSMFE, Rio de Janeiro.

Arthur, J.R.F. (1988). Cubical devices: Versatility and constraints. Advanced triaxial testing of soil and rock (eds R.T. Donaghe, R.C. Chaney and M.L. Silver) ASTM:STP977, 743-765.

Arthur, J.R.F., et al. (1977). Induced anisotropy in a sand. Geotechnique 27, 1, 13-30.

Atkinson, J.H., et al.(1989). Determination of soil stiffness parameters in stress path probing tests. Proc. 12th ICSMFE, Rio de Janeiro.

Baldi, G., et al.(1988). A reevaluation of conventional triaxial test methods. Advanced triaxial testing of soil and rock(eds R.T. Donaghe, R.C. Chaney and M.L. Silver) ASTM:STP 977, 219-263.
Baldi, G. and Nova, R. (1984). Membrane penetration effects in triaxial testing. J. Geotech. Eng., Proc. ASCE 110, 3, 403-420
Been, K. and Jefferies, M.G. (1985). A state parameter for sands. Geotechnique 35, 2, 99-112.
Been, K. and Jefferies, M.G. (1986). Discussion: A state parameter for sands. Geotechnique 36, 1, 127-132.
Been, K., et al. (1986). The cone penetration test in sands: part I, state parameter interpretation. Geotechnique 36, 2, 239-249.
Been, K., et al. (1987). The cone penetration test in sands: part II, general inference of state. Geotechnique 37, 3, 285-299.
Bellotti, R., et al. (1985). Laboratory validation of in-situ tests. Geotechnical engineering in Italy: An overview published on the occasion of golden jubliee of Int. Soc. of Soil Mech. & Foundn. Engineering, San Francisco.
Biarez, J., et al.(1989). Compressibility of Clayey Soils between 10^{1} and 10^{8} PA. Proc. 12th ICSMFE, Rio de Janeiro.
Bishop, A.W. and Wesley, L.D. (1975). A hydraulic triaxial apparatus for controlled stress path testing. Geotechnique 25, 4, 657-670.
Bjerrum, L. (1954). Theoretical and experimental investigations on the shear strength of soils, Norwegian Geotechnical Institute Publication No. 5. Oslo, Norway.
Blatt, H., et al. (1971). Origin of Sedimentary rocks. Prentice Hall Inc. Englewood Cliff, New Jersey, U.S.A.
Bolton, M.D. (1986). The strength and dilatancy of sands. Geotechnique 36, 1, 65-78.
Brady, K.C. (1988). Soil suction and the critical state. Geotechnique 38, 1, 117-120.
Brand, E.W. (1981). Some thoughts on rain-induced slope failures. Proc. 10th ICSMFE 3, 373-376, Stockholm.
Bressani, L.A. and Vaughan, P.R. (1989). Damage to soil structure during triaxial testing. Proc.12th ICSMFE, Rio de Janeiro.
Burmister, M.D. (1962). Physical stress-strain and strength response of granular soils. Symposium on field testing of soils. ASTM: STP 322.
Carrier III, W.D., and Beckman, J.F. (1984). Correlations between index tests and the properties of remoulded clays. Geotechnique (34), 2, 211-228.
Castro, G. (1969). Liquefaction of sands, Harvard Soil Mechanics Series, No.8. Pierce Hall, Cambridge Massachusetts, U.S.A.
Castro, G., et al. (1982). Liquefaction induced by cyclic loading. Report to National Science Foundation, Geotechnical Engieners Inc., Winchester, Massachusetts.
Clayton, C.R.I., et al. (1985). Dynamic penetration resistance and the prediction of the compressibility of a fine grain sand. Geotechnique 35, 1, 19-31.
Clayton, C.R.I. and Khatrush, S.A. (1986). A new device for measuring local axial strains on triaxial specimens Geotechnique 36, 4, 593-597.
Croney, D., and Coleman, J.D. (1954). Soil structure in relation to soil suction (PF). J. of soil science 5, 1.
Croney, D. (1977). The design & performance of road pavements. London: Her Majesty's stationary office.
Cundall, P.A. (1988). Computer simulations of dense sphere assemblies. Micromechanics of granular materials (eds. M. Satake and J.T. Jenkins), pp 113-123. Elsevier Science Publishers.
Desrues, J., et al. (1985). Localization of the formation in tests on sand sample. Engineering fracture mechanics 21, 4, 909-921.
Desrues, J. and Hammad, W. (1989). Experimental study of the localization of deformation on sand: influence of the mean stress. Proc. 12th ICSMFE, Rio de Janeiro.
Donaghe, R.T., et al. (1988). Advanced triaxial testing of soil and rock. ASTM: STP977.
Dumbleton, M.J., and West, G.(1970). The suction & strength of remoulded soils. Road Research Laboratory, Ministry of Transport, U.K. RRL Report LR 306.
Dyvik, R. and Madshus, C. (1985). Laboratory measurements of G_{max} using bender elements. Proc. ASCE Annual convention: Advances in the art of testing soils under cyclic conditions, Detroit (October).
Dyvik, R. and Olsen, T.S. (1989). G_{max} measured in oedometer and DSS tests using bender elements. Proc. 12th ICSMFE, Rio de Janeiro.
Egan, J.A. (1977). A critical state model for the cyclic loading pore pressure response of Soils, Master of Science Thesis presented to Cornell University at Ithaca, N.Y.
Eigenbrod, D.D., et al. (1987). Drained deformation and failure due to cyclic pore pressures in soft natural clay at low stresses. Canadian Geotechnical Journal 24, 2, 208-215.
Goldscheider, M.(1982). True triaxial tests on dense sand. In Results of the international workshop on constitutive relations, 11-54, A.A. Balkema, Rotterdam.
Griffiths, J.C. (1967). Scientific method in analysis of sediments. McGraw-Hill, N.Y., U.S.A.
Hambly, E.C. (1969). A new true triaxial apparatus. Geotechnique 19, 2, 307-309.
Hambly, E.C. and Roscoe, K.H. (1969). Observations and predictions of stresses and strains during plane strain of "wet" clays. Proc. 7th ICSMFE, 1, 173-181, Mexico.
Hardin, B.O. (1985). Crushing of soil particles. Proc. ASCE 111, 10, 1177-1192.
Hight, D.W., et al. (1983). The development of a new hollow cylinder apparatus for investigating the effects of principal stress rotation in soils. Geotechnique 33, 4, 355-383.
Hird, C.C. and Hassona, F.(1986). Discussion: A state parameter for sands. Geotechnique 36, 1, 124-127.
Hird, C.C. and Yung, P. (1987). Discussion: A new device for measuring local axial strains on triaxial specimens. Geotechnique 37, 3, 413-414.
Hofmann, F. (1939). Modern Castings, 35,125-128.
Holubec I. and E. D'Appolonia. (1973). Effect of particle shape on the engineering properties of granular Soils. Evaluation of relative density and its role in gotechnical projects involving cohesionless soils. ASTM: STP 523, 304-318.
Houlsby, G.T. (1981). A study of plasticity theories and their applicability to soils. PhD thesis, University of Cambridge.
Hutchinson, J.N. (1970). A coastal mudflow on the London clay cliffs at Beltinge, North

Kent. Geotechnique 20, 4, 412-438.
Ikegami, K. (1982). Experimental plasticity on the anisotropy of metals. In Mechanical behaviour of anisotropic solids. (ed. J.-P. Boehler) (Colloques Internationaux du Centre National de la Recherche Scient- ifique No. 295) Martinus Nijhoff Publishers/Editions du CNRS 201-242.
Imai, G. (1989). A unified theory of one dimensional consolidation with creep. Proc.12th ICSMFE, Rio de Janeiro.
Ishihara, K. and Watanabe, T. (1976). Sand liquefaction through volume decrease potential, Soils and Foundations 16, 6, 61-70.
Jamiolkowski, M., et al. (1985). New developments in field and laboratory testing of soils. Proc. 11th ICSMFE, 1, 57-153, San Francisco.
Jardine, R.J., et al. (1984). The measurement of soil stiffness in the triaxial apparatus. Geotechnique 34, 3, 323-340.
Jardine, R.J., et al. (1986). Studies of the influence of non-linear stress-strain characteristics in soil structure interaction. Geotechnique 36, 3, 377-396.
Kapoor, J.K. (1985). Compressibility and frictional resistance of a variety of sands. M. Tech thesis, IIT Kanpur, India.
Koerner, R.M. (1968). The behaviour of cohesionless soils formed from various minerals, Ph.D. thesis, Duke University, U.S.A.
Kolbuszewski, J.J. (1948). An experimental study of the maximum and minimum porosities of sands. Proc. 2nd ICSMFE, 1, 158-165, Rotterdam.
Kolisoja, P., et al. (1989). An automatic triaxial-oedometer device. Proc 12th ICSMFE, Rio de Janeiro.
Kolymbas, D. and Wu, W. (1989). Recent results of triaxial tests with grannular materials (submitted for publication).
Krumbein, W.C. (1941). Measurement of geological significance of shape and roundness of sedimentary particles. Journal Sedimentary Petrology, 11, 64-72.
Ladd, C.C., et al (1977). Stress-deformation and strength characteristics. Proc. 9th ICSMFE, 2, 421-494, Tokyo.
Ladd. C.C. (1981). Discussion: Laboratory shear devices. Proc. Symposium on Laboratory Shear Strength of soils (eds. R.N. Yong and F.C. Townsend), ASTM: STP 740, pp. 643-652.
Lade, P.V. and Hernandez, S.B. (1977). Membrane penetration effects in undrained tests. Proc. ASCE 103, GT2, 109-125.
Lambe, T.W. (1967). Stress path method. Proc. ASCE 93, SM6, 309-331.
Lee, K.L., and Farhoomand, I. (1967). Compressibility and crushing of granular soils in anisotropic triaxial compression. Can. Geotech. J. 4, 1, 68-99.
Lee, K.L. and Seed, H.B. (1967). Drained strength characteristics of sands. Proc. ASCE 93, SM6, 117-141.
Lees, G. (1964). The measurement of particle shape and its influence in engineering materials. J. British Granite and Whinstone Federation 4, 2.
Leroueil, S., et al. (1983). Proprietes Characteristiques des argiles de l'est du Canada. Can. Geotech. J. 20, 4, 681-705.
Leroueil, S., et al. (1985). Discussion: Correlations between index tests and the properties of remoulded clays. Geotechnique 35, 2, 223 - 226.
Leroueil, S., et al. (1985a). Remblais surargiles molles. Technique et Documentation (Lavoisier).
Leroueil, S., et al. (1985b). Stress-strain-strain rate relation for the compressibility of sensitive natural clays. Geotechnique 35, 2, 159-180.
Leroueil, S., et al. (1986). Discussion closure: Stress-strain-strain rate relation for the compressibility of sensitive natural clays. Geotechnique 36, 2, 288-290.
Li, X.S., et al. (1988). An automated triaxial testing system. Advanced triaxial testing of soil and rock (eds. R.T. Donaghe, R.C. Chaney and M.L. Silver) ASTM: STP 977, 95-106.
Matsuoka, H., et al. (1989). "General stress" tests on granular materials. Proc. 12th ICSMFE, Rio de Janeiro.
Mayne, P.W. (1980). Cam-clay predictions of undrained strength. Proc. ASCE 106, GT11, 1219 - 1242.
Mayne, P.W., and Swanson, P.G. (1981). The critical-state pore pressure parameter from consolidated undrained shear tests. Laboratory shear strength of soils (eds. R.N. Yong and F.C. Townsend) ASTM: STP 740, 410-430.
Menzies, B.K. (1988). A computer controlled hydraulic triaxial testing system. Advanced triaxial testing of soil and rock (eds. R.T. Donaghe, R.C. Chaney and M.L. Silver) ASTM: STP 977, 82-94.
Mesri, G. and Feng, T.W. (1986). Discussion: Stress-strain-strain rate relation for the compressibility of sensitive natural clays. Geotechnique 36, 2, 283-287.
Mitchell, J.K. (1976). Fundamentals of soil behaviour. John Wiley & Sons.
Negussey, D., et al. (1988). Constant-volume friction angle of granular materials. Canadian Geotechnial J. 25, 1, 50-55.
NRC 1985). Liquefaction of Soils during earthquakes. National academy press, Washington, D.C., U.S.A.
Oda, M., et al. (1985). Stress-induced anisotropy in granular masses. Soils and Foundations 25, 3, 85-97.
Olli, R., et al. (1989) Versatile triaxial equipment in the University of Oulu. Proc. 12th ICSMFE, Rio de Janeiro.
Parry, R.H.G. and Wood, D.M.(1982). Stress States, stress paths and critical states for soils. Lecture notes 5, Cambridge University, Engineering Department, U.K.
Pietruszczak, S. and Pande, G.N. (eds). (1985). Numerical models in geomechanics NUMOG III, Elsevier Applied Science.
Powers M.C. (1953). A new roundness scale for sedimentary particles. Journal of Sedimentary Petrology 23, 2, 117-119.
Rahim, A. (1989). Effect of morphology and mineralogy on compressibility of sands. Ph.D.thesis submitted to IIT Kanpur, India.
Roscoe, K.H., et al. (1958). On the yielding of soils. Geotechnique 8, 1, 22-52.
Roscoe, K.H. and Burland, J.B. (1968) On the generalised stress-strain behaviour of "wet" clay. Engineering Plasticity, (eds. J. Heyman and F.A. Leckie) , 535-609, Cambridge University Press.
Rowe, P.W. and Barden, L. (1964). Importance of free ends in triaxial testing. Proc. ASCE 90, SM1, 1-27.
Saada, A.S. and Bianchini, G.F. (1977). Discussion closure: Strength of one dimensionally

consolidated clays. Proc. ASCE 103, GT6, 655-660.
Sayao, A.S.F. and Vaid, Y.P. (1989). Deformations due to principal stress rotation. Proc. 12th ICSMFE, Rio de Janeiro.
Schofield, A.N. and Wroth, C.P. (1968). Critical State Soil Mechanics. McGraw-Hill, London.
Schofield, A.N. (1980). The Cambridge geotechnical centrifuge operations: 20th Rankine lecture. Geotechnique 30, 3, 227-268.
Seed, R.B., et al. (1989). Elimination of membrane compliance effects in undrained testing. Proc. 12th ICSMFE, Rio de Janeiro.
Seed, H.B. et al.(1964). Fundatmental aspects of the Atterberg limits. Proc. ASCE, 90, SM6 75-105.
Shen, C.K., et al.(1989). Microcomputer based laboratory apparatus for soil testing. Proc. 12th ICSMFE, Rio de Janeiro.
Shibuya, S., and Hight, D.W. (1989). Predictions of pore pressure under undrained cyclic principal stress rotation. Proc. 12th ICSMFE, Rio de Janeiro.
Skempton, A.W. (1953). Soil mechanics in relation to geology. Proc. Yorkshire Geological Society, 29, 33-62.
Skempton, A.W., and Northey, R.D. (1952). The sensitivity of clays. Geotechnique 3, 1, 30-53.
Sladen, J.A. and Handford, G, (1987). A potential systematic error in laboratory testing of very loose sand. Canadian Geotechnical Journal 24, 3, 462-466.
Smart, P. and Tovey, N.K. (1988). Micorfabric of the deformation of soils. Report to AFOSR (grant 87-0346).
Stroud, M.A. (1971) The behaviour of sand at low stress levels in the simple shear apparatus. PhD Thesis, Cambridge University.
Sture, S., et al. (1985). Development and application of a directional shear cell. Proc. 11th ICSMFE 2, 1061-1064, San Francisco.
Sture. S., et al. (1988). True triaxial and directional shear cell experiments on dry sand. Final report GL-88-1 to Department of the Army, US Army Corps of Engineers.
Swoboda, G. (ed.) (1988). Numerical methods in geomechanics, Proc. 6th Int. Conf. on Numerical Methods in Geomechanics. Innsbruck, A.A. Balkema, Rotterdam.
Tatsuoka, F. (1988). Some recent developments in triaxial testing systems for cohesionless soils. Advanced triaxial testing of soil and rock (eds R.T. Donaghe, R.C. Chaney and M.L. Silver) ASTM:STP 977, 7-67.
Topolnicki, M. (1989). On shear strength of normally consolidated and saturated clay. Proc. 12th ICSMFE Rio de Janeiro.
Vaid, Y.P., and Chern, J.C. (1985). Cyclic and monotonic response of saturated sands. Proc. ASCE Annual Convention: Advances in the art of testing soils under cylic conditions, Detroit, Mechigan (October).
Vaid, Y.P., et al. (1988). A stress and strain-controlled monotonic and cyclic loading system. Advanced triaxial testing of soil and rock. (eds. R.T. Donaghe, R.C. Chaney and M.L. Silver.) ASTM: STP 977, 119-131.
Van Impe, W.F. and Van den Broeck, M. (1989). Developments and modelling of the free torsion pendulum test. Proc. 12th ICSMFE, Rio de Janeiro.
Vardoulakis, I. (1988). Theoretical and experimental bounds for shear-band bifurcation strain in biaxial tests on dry sand. Res Mechanica 23, 239-259.
Wadell, H. (1932). Volume, shape, roundness of quartz pebbles. Journal of geology 40, 443-451.
Wilson, J.M.R. (1988). A theoretical and experimental investigation into the dynamic behaviour of soils. PhD thesis, Cambridge University.
Winterkorn, H.F. and Fang, H.Y. (1975). Foundation engineering handbook. Van Nostrand Reinhold.
Wong, R.K.S., et al. (1987). Induced anisotropy in wet remoulded kaolinite and bentonite model materials. Chemical Engineering Science 42, 4, 745-751.
Wood, D.M., et al. (1979). On the determination of the stress state in the simple shear apparatus. Geotechnical Testing Journal, ASTM 2, 4, 211-222.
Wroth, C.P. and Wood, D.M. (1978). The correlation of index properties with some basic engineering properties of soils. Can. Geotech. J. 15, 2, 137-145.
Wroth, C.P. (1984) The interpretation of in situ soil tests (24th Rankine lecture). Geotechnique 34, 4, 449 - 489.
Yin, J.H., et al. (1989). Constitutive modelling of soil behaviour using three modulus hypoelasticity. Proc. 12th ICSMFE, Rio de Janeiro.
Youd, L. (1973). Factors Controlling maximum and minimum densities of sands. Evaluation of relative density and its role in geotechnical projects involving cohesionless soils. ASTM: STP 523, 98-112.
Yudhbir. and Rahim, A.(1987). Compressibility characteristics of sands. Proc. 9th SEAGC 1, 483-494, Bangkok.
Zingg, T. (1935). Beitrage zur Schotteranalyse. Schweiz, Min. Pet. Mitt. (15), 39-140.

APPENDIX

Papers submitted to session 1: Recent developments in laboratory strength and deformation testing.

1. ANSAL, TUNCAN. Consolidation in clays due to cyclic stresses.
2. ATKINSON, LAU, POWELL. Determination of soil stiffness parameters in stress path probing tests.
3. BALASUBRAMANIAM, HANDALI, PHIENWEJA, KUWANO. Pore pressure stress ratio relationship for soft clay.
4. BIAREZ, FLEUREAU, ZERHOUNI. Compressibility of clayey soils between 10^1 and 10^8 PA.
5. BRESSANI, VAUGAN. Damage to soil structure during triaxial testing.
6. CARDOSO-MAJ. Resilient modulus predictive equation based on permanent deformation tests.
7. CAMAPUM DE CARVALHO, CRISPEL, MIEUSSENS. Mechanical behaviour of compacted marl.
8. CHEHADE, ROBINET, SHAHROUR. Dilatancy and liquefaction criterion in triaxial and torsion tests.
9. DESRUES, HAMMAD. Experimental study of the localization of deformation on sand: influence of the mean stress.
10. DIAZ-RODRIGUEZ, LEYTE-GUERRERO. Consolid-

ation of Mexico City clay under repeated loading.
11. DYVIK, OLSEN: G_{max} measured in oedometer and DSS tests using bender elements.
12. ESCARIO, JUCA. Strength and deformation of partly saturated soils.
13. HABERFIELD, JOHNSTON. Relationship between fracture toughness and tensile strength for geomaterials.
14. HORTA. Carbonate and gypsum soils properties and classification.
15. IMAI. A unified theory of one dimensional consolidation with creep.
16. KOLISOJA, SAHI, HARTIKAINEN. An automatic triaxial-oedometer device.
17. MATSUOKA, SUZUKI, MURATA. "General stress" tests on granular materials.
18. MIEUSSENS, NARDONE, GHLISS. Oedometer suction controlled tests.
19. OHTA, NISHIHARA, IIZUKA, MORITA, FUKAGAWA, ARAI. Unconfined compression strength of soft aged clays.
20. OLLI, KAUKO, VESA. Versatile triaxial equipment in the University of Oulu.
21. OSHO. Influence of electrolytes on stress strain behaviour of Kaolin.
22. PAPA, SILVESTRI, VINALE. Cyclic/dynamic simple shear tests: recent developments.
23. PUCCINI, SAADA, BIANCHINI. Validation of failure models for granular soils.
24. RIZKALLAH, KEESE. Geotechnical properties of collapsible soils.
25. SALLFORS. Quality assurance in laboratory testing.
26. SAYAO, VAID. Deformations due to principal stress rotation.
27. SEED, ANWAR, NICHOLSON. Elimination of membrane compliance effects in undrained testing.
28. SENNESET. A new oedometer with splitted ring for the measurement of lateral stress.
29. SHEN, LI, CHAN, WANG. Microcomputer based laboratory apparatus for soil testing.
30. SHIBUYA, HIGHT. Predictions of pore pressure under undrained cyclic principal stress rotation.
31. TOPOLNICKI. On shear strength of normally consolidated and saturated clay.
32. VAN IMPE, VAN DEN BROECK. Developments and modelling of the free torsion pendulum test.
33. WEI, SUN, WAGN. Pore pressure behaviour of soft clay.
34. YIN, GRAHAM, SAADAT, AZIZI. Constitutive modelling of soft soil behaviour using three modulus hypoelasticity.

ACKNOWLEDGEMENTS

Help and facilities so liberally provided by the Indian Institute of Technology, Kanpur; Asian Institute of Technology, Bangkok and Glasgow University, Scotland are gratefully acknowledged. The senior author would like to thank President A.M. North, Professors Prinya Nutalaya and A.S. Balasubramaniam at AIT for all the help and facilities in the preparation of this report. Useful discussions with Professor A.S. Balasubramaniam at AIT and Professor M. R. Madhav at IIT are appreciated. Professor S.T. Wong (Visiting faculty at AIT) from Simon Fraser University, Canada, provided very valuable insight to the senior author in the analysis of data.

The untiring efforts of Mrs. Uraivan S. and Mrs. Vatinee C. are highly appreciated for the physical preparation of the report.